Nucleosintesi oltre il picco del Fe. Misure di cattura neutronica di interesse Astrofisico

Introduction: Nuclear Astrophysics

"the majority of the chemical elements in the universe is produced through nuclear reactions in the hot interiors of the stars"

REVIEWS OF
MODERN PHYSICS

VOLUME 29, NUMBER 4 — OCTOBER, 1957

Synthesis of the Elements in Stars*

E. MARGARET BURBIDGE, G. R. BURBIDGE, WILLIAM A. FOWLER, AND F. HOYLE

Kellogg Radiation Laboratory, California Institute of Technology, and Mount Wilson and Palomar Observatories, Carnegie Institution of Washington, California Institute of Technology, Pasadena, California

"It is the stars, The stars above us, govern our conditions";
(*King Lear*, Act IV, Scene 3)

but perhaps

"The fault, dear Brutus, is not in our stars, But in ourselves,"
(*Julius Caesar*, Act I, Scene 2)

Introduction: Nuclear Astrophysics

EXPERIMENTAL AND THEORETICAL NUCLEAR ASTROPHYSICS; THE QUEST FOR THE ORIGIN OF THE ELEMENTS

Nobel lecture, 8 December, 1983

by

WILLIAM A. FOWLER

W. K. Kellogg Radiation Laboratory

California Institute of Technology, Pasadena, California 91125

Ad astra per aspera et per ludum

SCIENCE volume 225 (1984) 922

Abundances beyond Fe–ashes of stellar burning

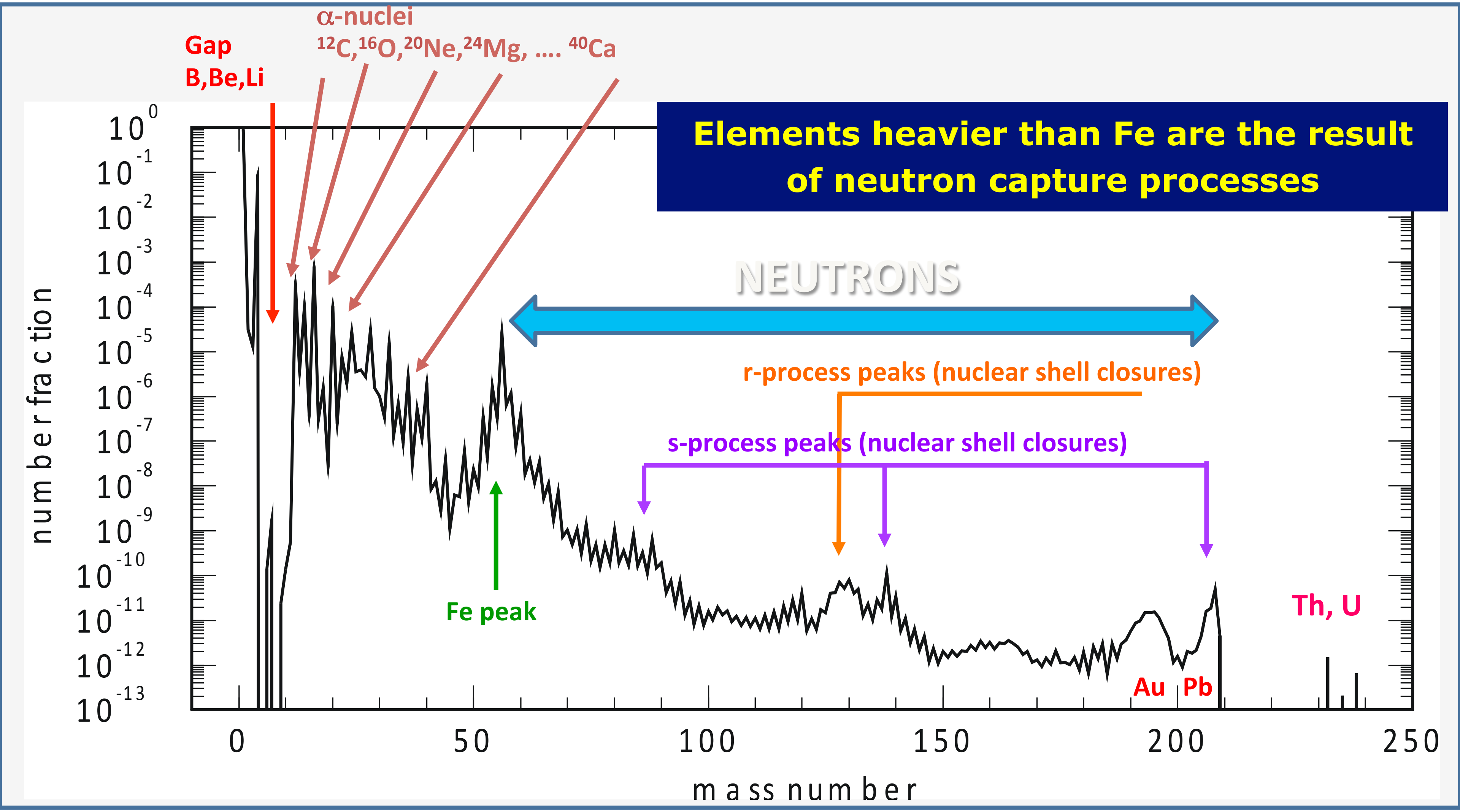

Nucleosynthesis

s-process lifetime 10^4 years $n_n \approx 10^8$ neutron/cm^3

r-process lifetime μs $n_n \approx 10^{22}$ neutron/cm^3

β-decay lifetime: few hours to some months

The canonical s-process

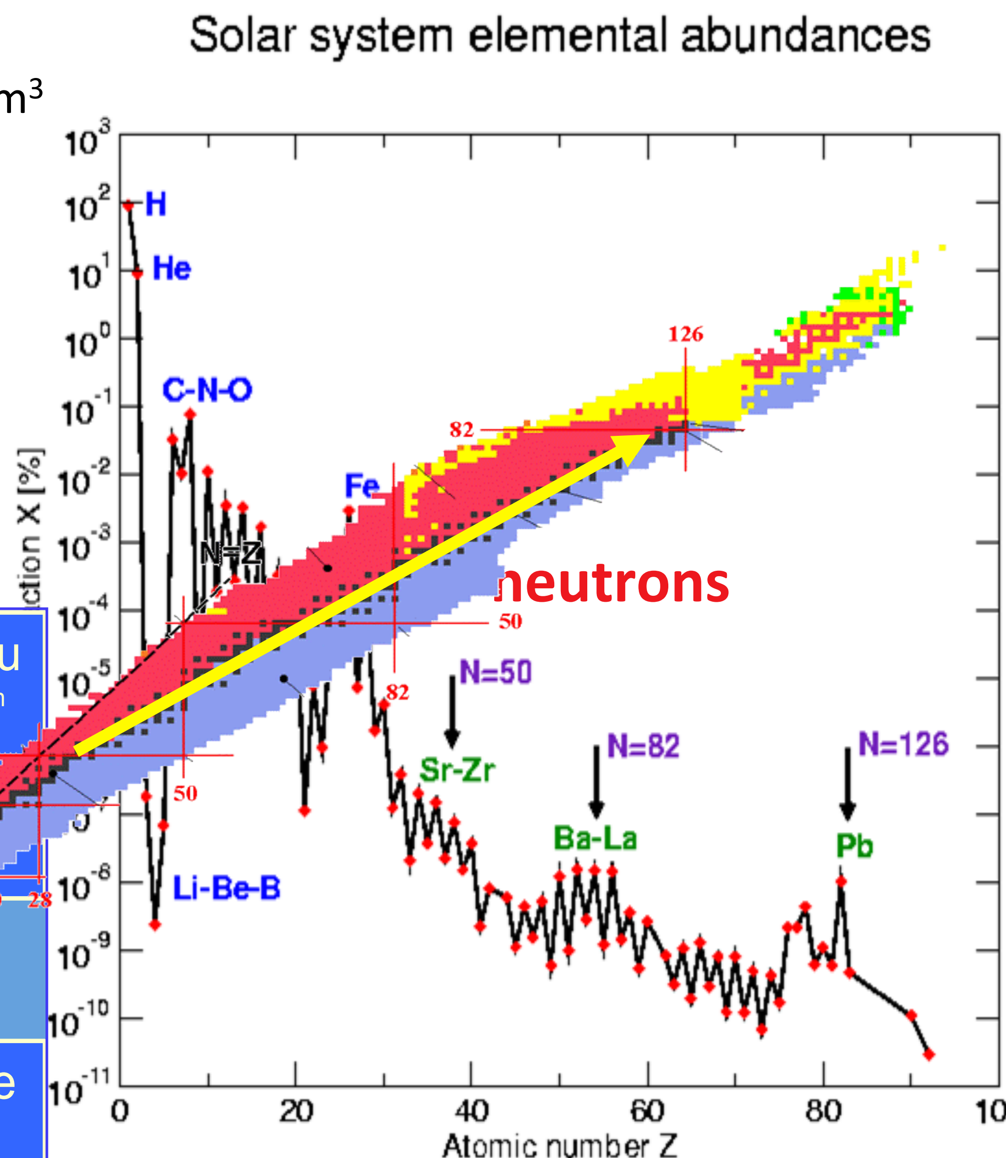

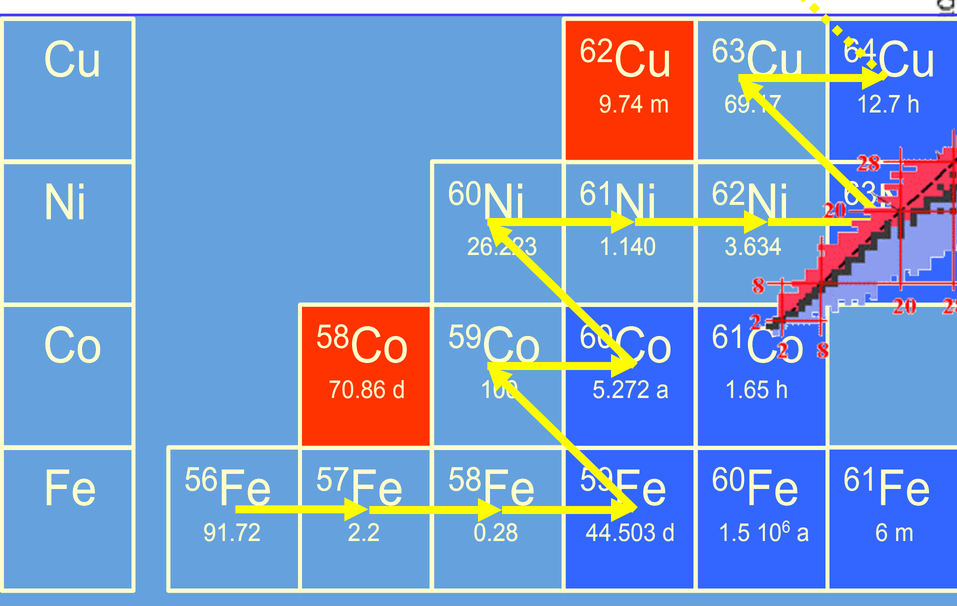

Nucleosynthesis in the r-process

JINA

Joint Institute for Nuclear Astrophysics 2002

Movie : H. Schatz, National Superconducting Cyclotron Laboratory

Calculation : K. Vaughan, J.L. Galache, and A. Aprahamian, University of Notre Dame

Model : B. Meyer, Clemson University and R. Surman, North Carolina State

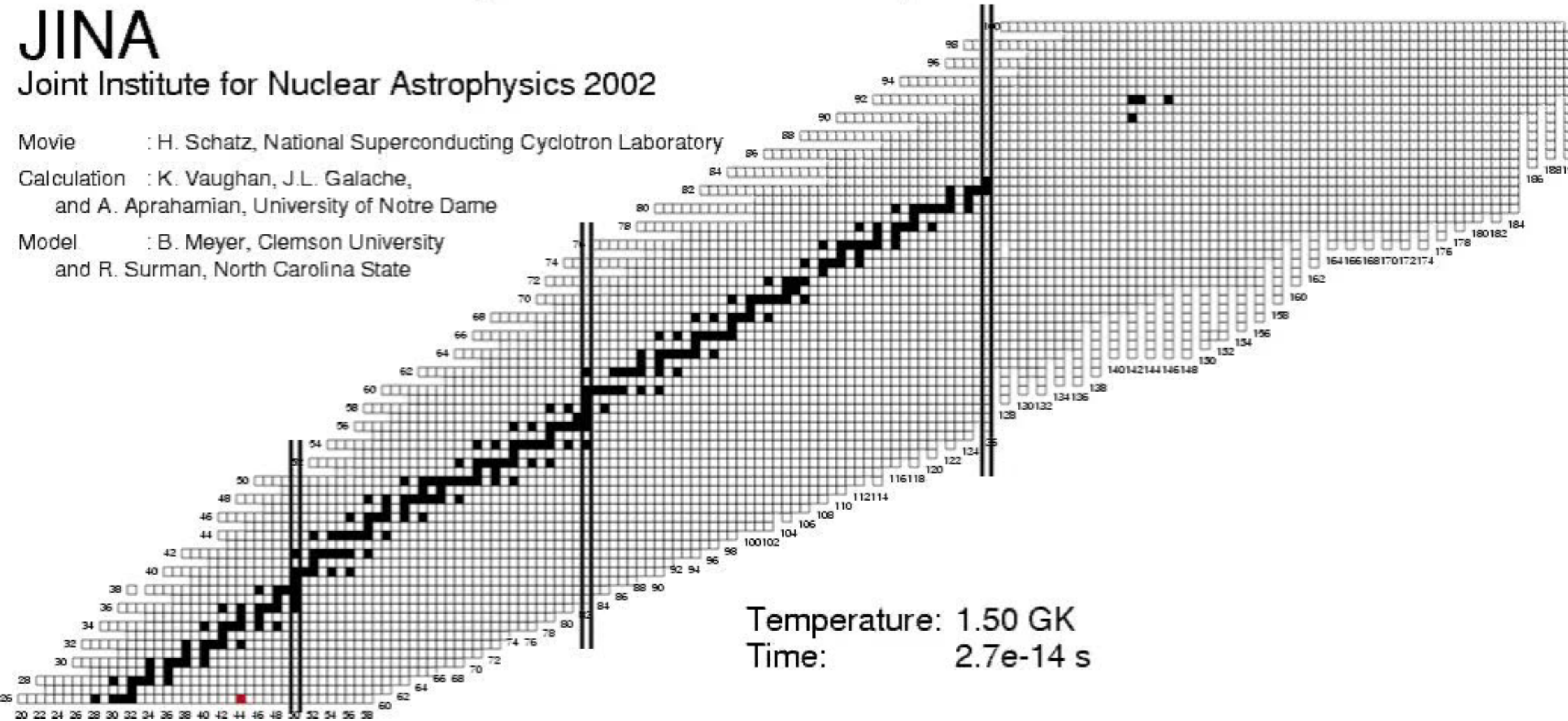

Temperature: 1.50 GK

Time: 2.7e-14 s

processo-p

La maggiore parte degli elementi più pesanti del Fe vengono sintetizzati tramite cattura neutronica. Ci sono, comunque, 35 elementi in cui il numero di protoni è maggiore del numero di neutroni

Nucleus	Z	Solar system abundance ($Si = 10^6$)	Isotopic abundance (%)	Nucleus	Z	Solar system abundance ($Si = 10^6$)	Isotopic abundance (%)
^{74}Se	34	$5.5 \cdot 10^{-1}$	0.88	^{132}Ba	56	$4.53 \cdot 10^{-3}$	0.1
^{78}Kr	36	$1.53 \cdot 10^{-1}$	0.34	^{138}La	57	$4.09 \cdot 10^{-4}$	0.09
^{84}Sr	38	$1.32 \cdot 10^{-1}$	0.56	^{136}Ce	58	$2.16 \cdot 10^{-3}$	0.19
^{92}Mo	42	$3.78 \cdot 10^{-1}$	14.84	^{138}Ce	58	$2.84 \cdot 10^{-3}$	0.25
^{94}Mo	42	$2.36 \cdot 10^{-1}$	9.25	^{144}Sm	62	$8.0 \cdot 10^{-3}$	3.1
^{96}Ru	44	$1.03 \cdot 10^{-1}$	5.52	^{152}Gd	64	$6.6 \cdot 10^{-4}$	0.2
^{98}Ru	44	$3.50 \cdot 10^{-2}$	1.88	^{156}Dy	66	$2.21 \cdot 10^{-4}$	0.06
^{102}Pd	46	$1.42 \cdot 10^{-2}$	1.02	^{158}Dy	66	$3.78 \cdot 10^{-4}$	0.10
^{106}Cd	48	$2.01 \cdot 10^{-2}$	1.25	^{162}Er	68	$3.51 \cdot 10^{-4}$	0.14
^{108}Cd	48	$1.43 \cdot 10^{-2}$	0.89	^{164}Er	68	$4.04 \cdot 10^{-3}$	1.61
^{113}In	49	$7.9 \cdot 10^{-3}$	4.3	^{168}Yb	70	$3.22 \cdot 10^{-4}$	0.13
^{112}Sn	50	$3.72 \cdot 10^{-2}$	0.97	^{174}Hf	72	$2.49 \cdot 10^{-4}$	0.16
^{114}Sn	50	$2.52 \cdot 10^{-2}$	0.66	^{180}Ta	73	$2.48 \cdot 10^{-6}$	0.01
^{115}Sn	50	$1.29 \cdot 10^{-2}$	0.34	^{180}W	74	$1.73 \cdot 10^{-4}$	0.13
^{120}Te	52	$4.3 \cdot 10^{-3}$	0.09	^{184}Os	76	$1.22 \cdot 10^{-4}$	0.02
^{124}Xe	54	$5.71 \cdot 10^{-3}$	0.12	^{190}Pt	78	$1.7 \cdot 10^{-4}$	0.01
^{126}Xe	54	$5.09 \cdot 10^{-3}$	0.11	^{196}Hg	80	$5.2 \cdot 10^{-4}$	0.15
^{130}Ba	56	$4.76 \cdot 10^{-3}$	0.11				

processo-p

Le abbondanze degli p-isotopi è molto bassa rispetto agli altri isotopi (1-0.1%) eccetto per gli isotopi $^{92,94}Mo$ e ^{96}Ru.
Si ipotizza lche gli isotopi s e r sono utilizzati come nuclei seme per il processi-p.

Molto probabilmente il processo-p ha luogo negli strati O/Ne delle supernove di tipo II, durante la fase esplosiva

s-only & r-only istopes

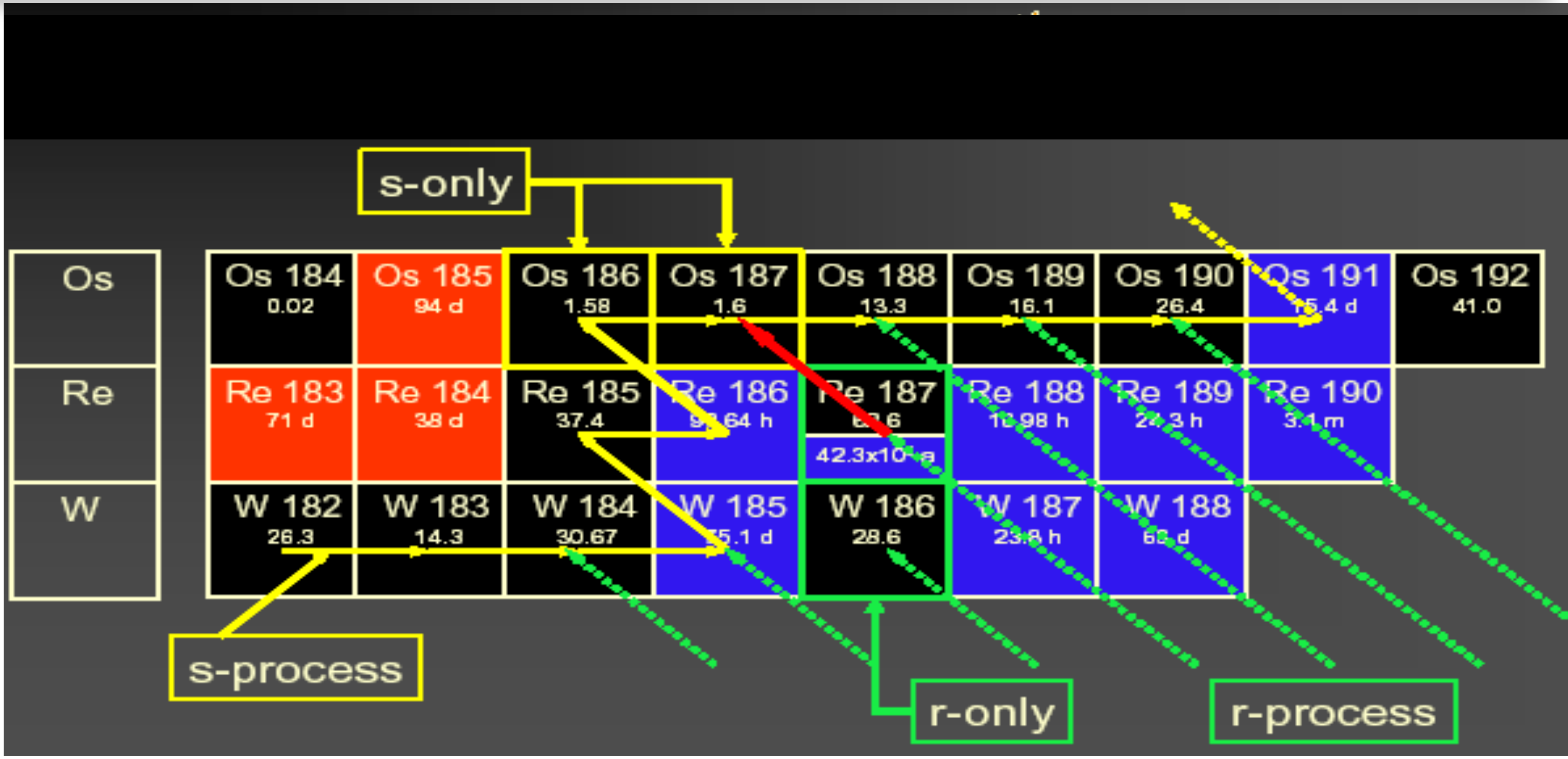

Stellar Models: local equilibrium approximation

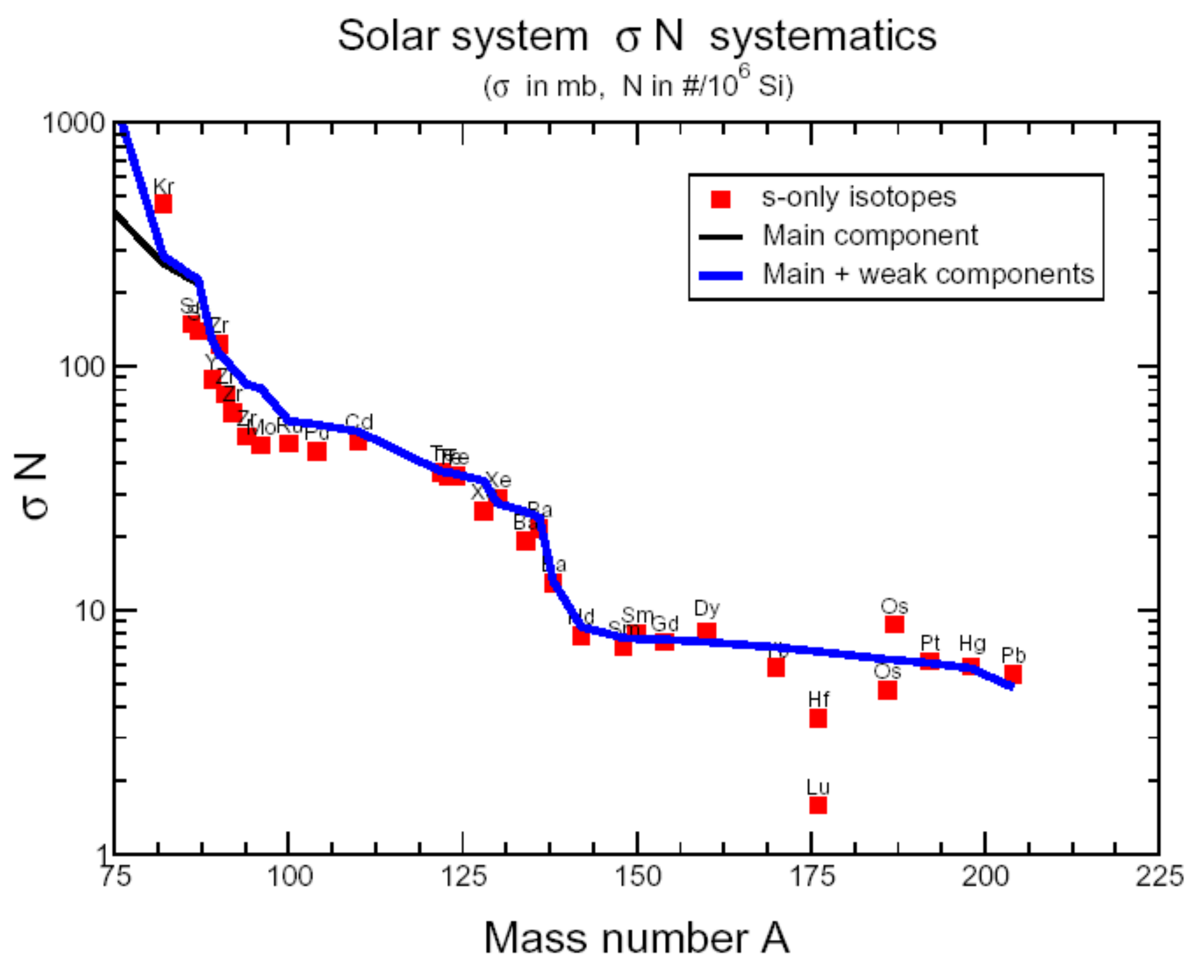

$$\sigma_A N_A = \cos t$$

$$\langle\sigma\rangle_A N_s(A) = \frac{f N_s^{seed}}{\tau_0} \prod_{i=56}^{A} \frac{1}{\left[1 + \frac{1}{\tau_0 \langle\sigma\rangle_i}\right]}$$

Stellar Models: Standard stellar model

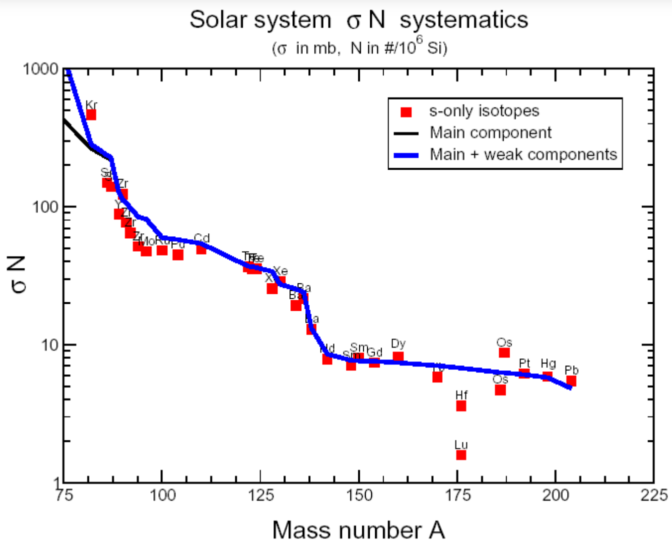

$$\langle\sigma\rangle_A N_s(A) = \frac{f N_s^{seed}}{\tau_0} \prod_{i=56}^{A} \frac{1}{\left[1 + \frac{1}{\tau_0 \langle\sigma\rangle_i}\right]}$$

f the fraction of ^{56}Fe seed nuclei that are subjected to an exposure of neutron

τ neutron exposure proportional to the time-integrated neutron flux

THE ASTROPHYSICAL JOURNAL, 354:630–643, 1990 May 10

s-PROCESS NUCLEOSYNTHESIS: CLASSICAL APPROACH AND ASYMPTOTIC GIANT BRANCH MODELS FOR LOW-MASS STARS

F. KÄPPELER
Kernforschungszentrum Karlsruhe, Institut für Kernphysik
R. GALLINO
Istituto di Fisica Generale dell' Università di Torino
M. BUSSO AND G. PICCHIO
Osservatorio Astronomico di Torino
AND
C. M. RAITERI
International School for Advanced Studies, Trieste

Received 1989 August 9; accepted 1989 November 15

Stellar Models: Standard stellar model

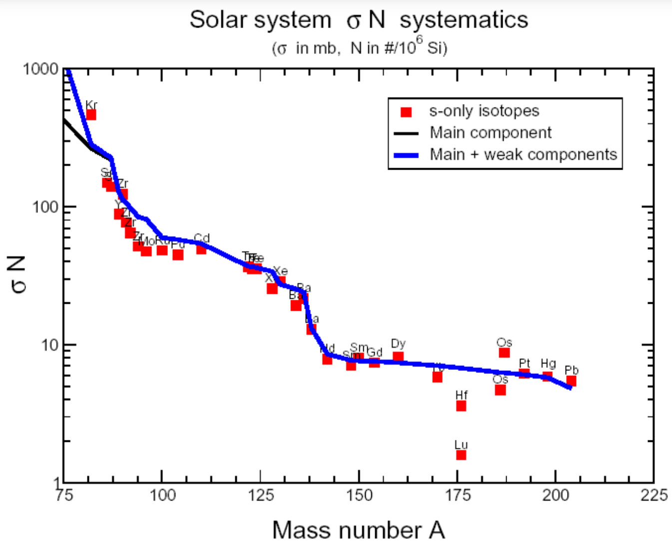

$$\langle\sigma\rangle_A N_s(A) = \frac{f N_s^{seed}}{\tau_0} \prod_{i=56}^{A} \frac{1}{\left[1 + \frac{1}{\tau_0 \langle\sigma\rangle_i}\right]}$$

f the fraction of ^{56}Fe seed nuclei that are subjected to an exposure of neutron
τ neutron exposure proportional to the time-integrated neutron flux

Main component: A = 90 -205, f ≈ 0.06%, τ ≈ 0.3 mb^{-1} → n_c = 10

Weak co

PERGAMON

Progress in Particle and Nuclear Physics 43 (1999) 419–483

Progress in Particle and Nuclear Physics

http://www.elsevier.nl/locate/ppartnuclphys

The Origin of the Heavy Elements: The *s* Process

F. KÄPPELER

Forschungszentrum Karlsruhe, Institut für Kernphysik, D-76021 Karlsruhe, Germany

Stellar Models: Standard stellar model

Annu. Rev. Astron. Astrophys. 1999. 37:239–309

NUCLEOSYNTHESIS IN ASYMPTOTIC GIANT BRANCH STARS: Relevance for Galactic Enrichment and Solar System Formation

M. Busso,[1] R. Gallino,[2] and G. J. Wasserburg[3]

[1]*Osservatorio Astronomico di Torino, 10025 Pino Torinese, Italy, e-mail: busso@to.astro.it;* [2]*Dipartimento di Fisica Generale, Universita' di Torino, Via P. Giuria 1, 10125 Torino, Italy, e-mail: gallino@ph.unito.it;* [3]*Lunatic Asylum, Division of Geological and Planetary Sciences, California Institute of Technology, Pasadena California 91125, e-mail: isotopes@gps.caltech.edu*

s-process stellar sites

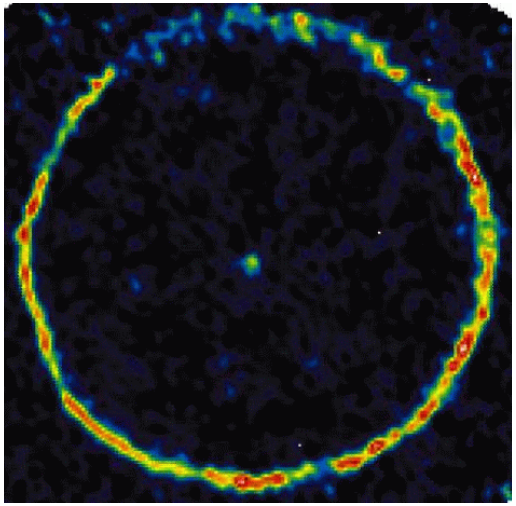

Low mass Asympotic Giant Branch (AGB) $M \approx 1.5$ - 3 $M_\odot$

- $^{13}C(\alpha,n)^{16}O$ T ~ 8 keV $N_n < 10^7$ n/cm^3
- $^{22}Ne(\alpha,n)^{25}Mg$ T ~ 23 keV N_n~10^{10}-10^{12} n/cm^3

Massive stars $M \approx 15$ - 25 $M_\odot$

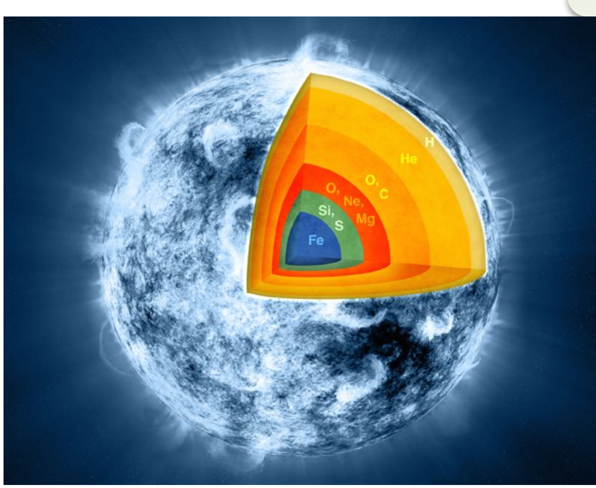

$^{22}Ne(\alpha,n)^{25}Mg$

In core He-burning T ~ 26 keV N_n ~ 10^6 n/cm^3

In core C-burnig T ~ 90 keV N_n~10^{11} n/cm^3

Asympotic Giant Branch (AGB)

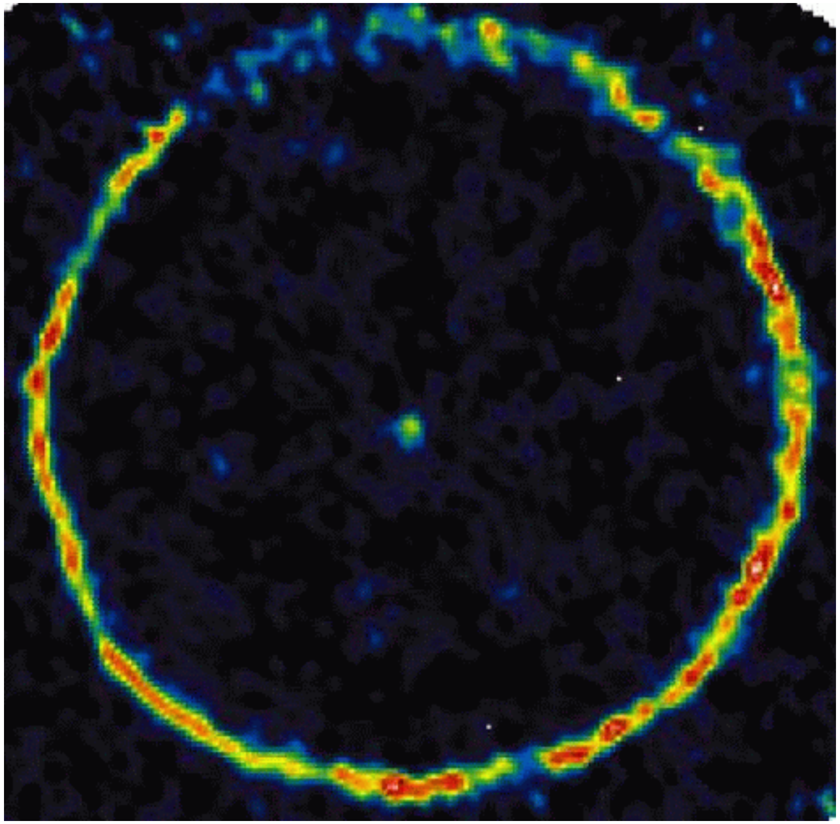

False-color picture of CO molecules tracing material around the AGB star TT-Cygni

Asympotic Giant Branch (AGB)

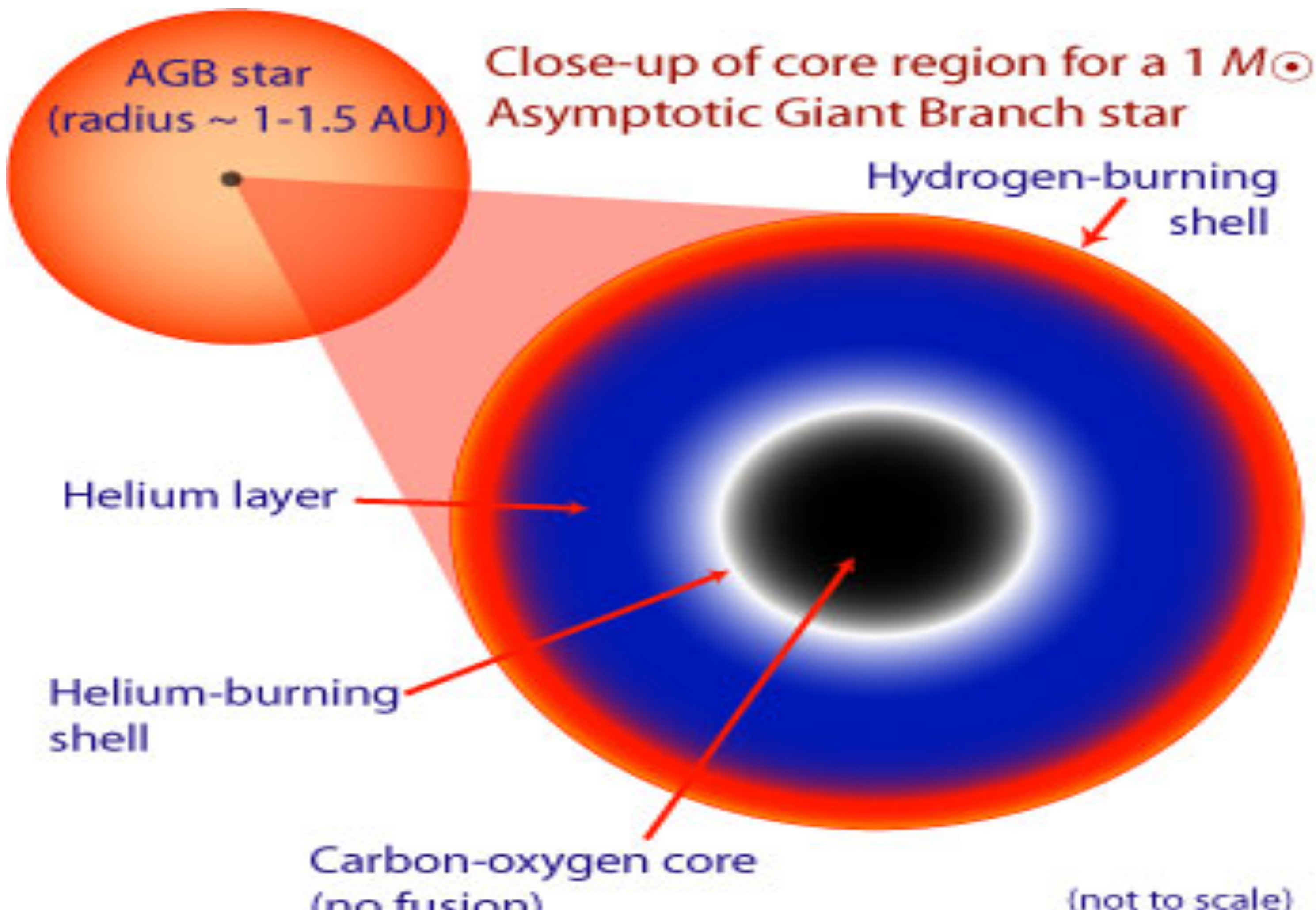

The TP Stellar Model

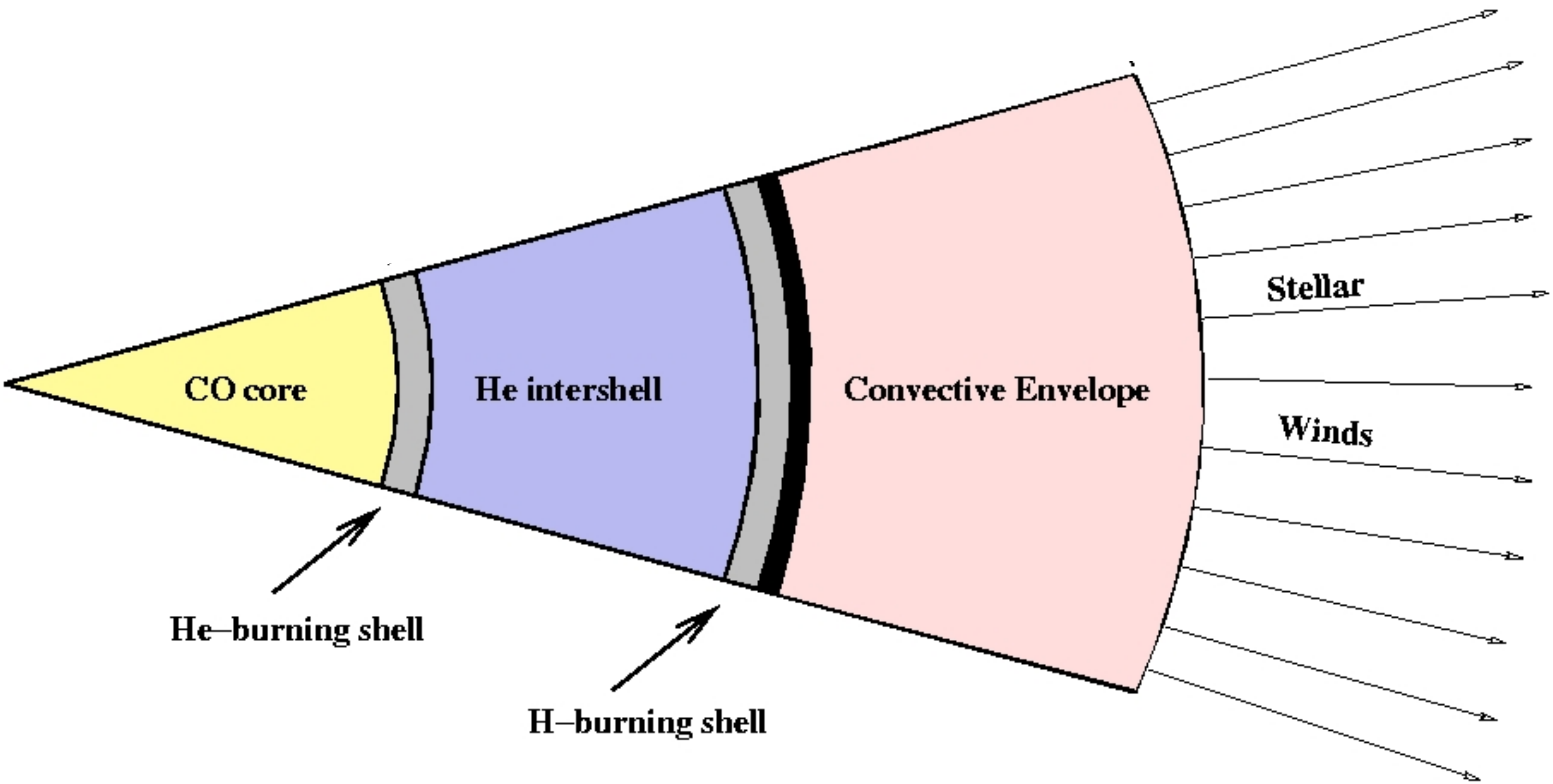

Schematic **out-of-scale** picture of the structure of AGB stars.

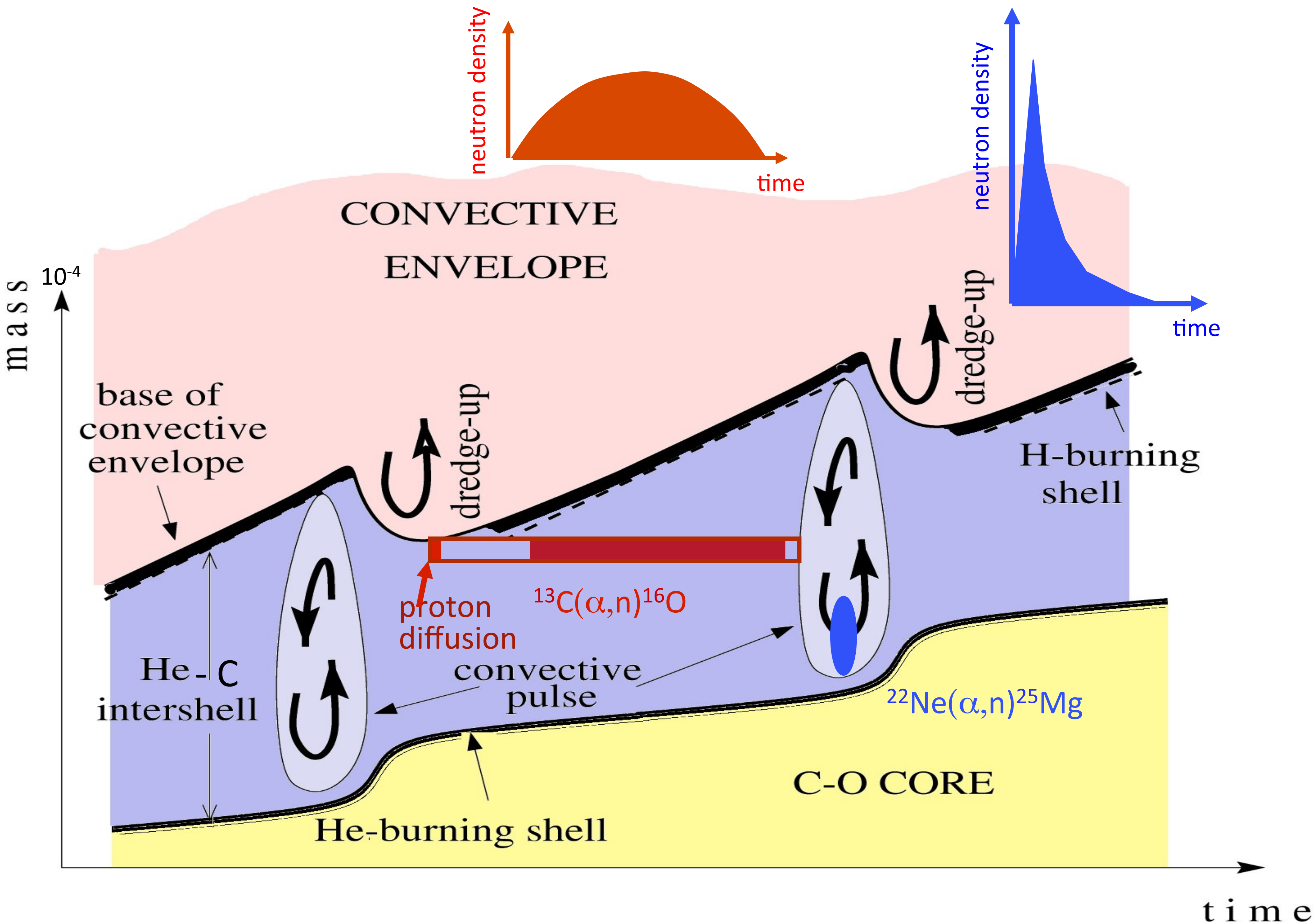

neutron density
time
neutron density
time
CONVECTIVE ENVELOPE
mass
10-4
base of convective envelope
dredge-up
dredge-up
H-burning shell
proton diffusion
13C(α,n)16O
He-C intershell
convective pulse
22Ne(α,n)25Mg
C-O CORE
He-burning shell
time

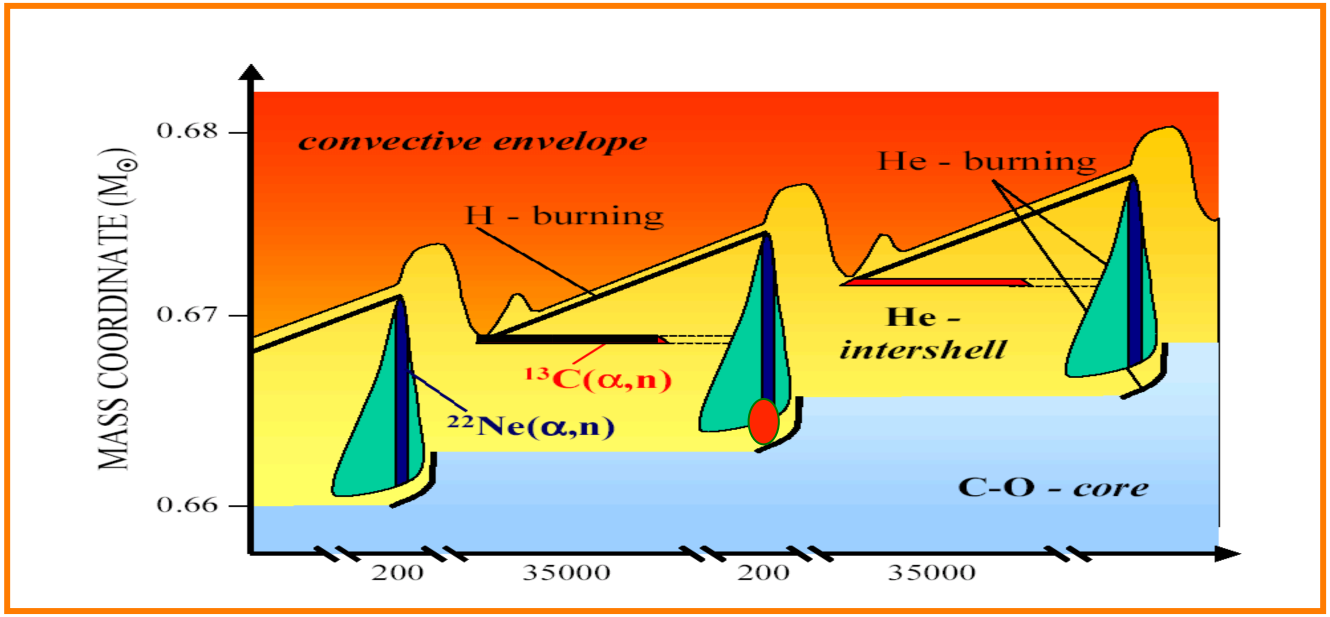

MASS COORDINATE ($M_\odot$)
0.68
0.67
0.66
convective envelope
H - burning
He - burning
He - intershell
$^{13}C(\alpha,n)$
$^{22}Ne(\alpha,n)$
C-O - core
200
35000
200
35000

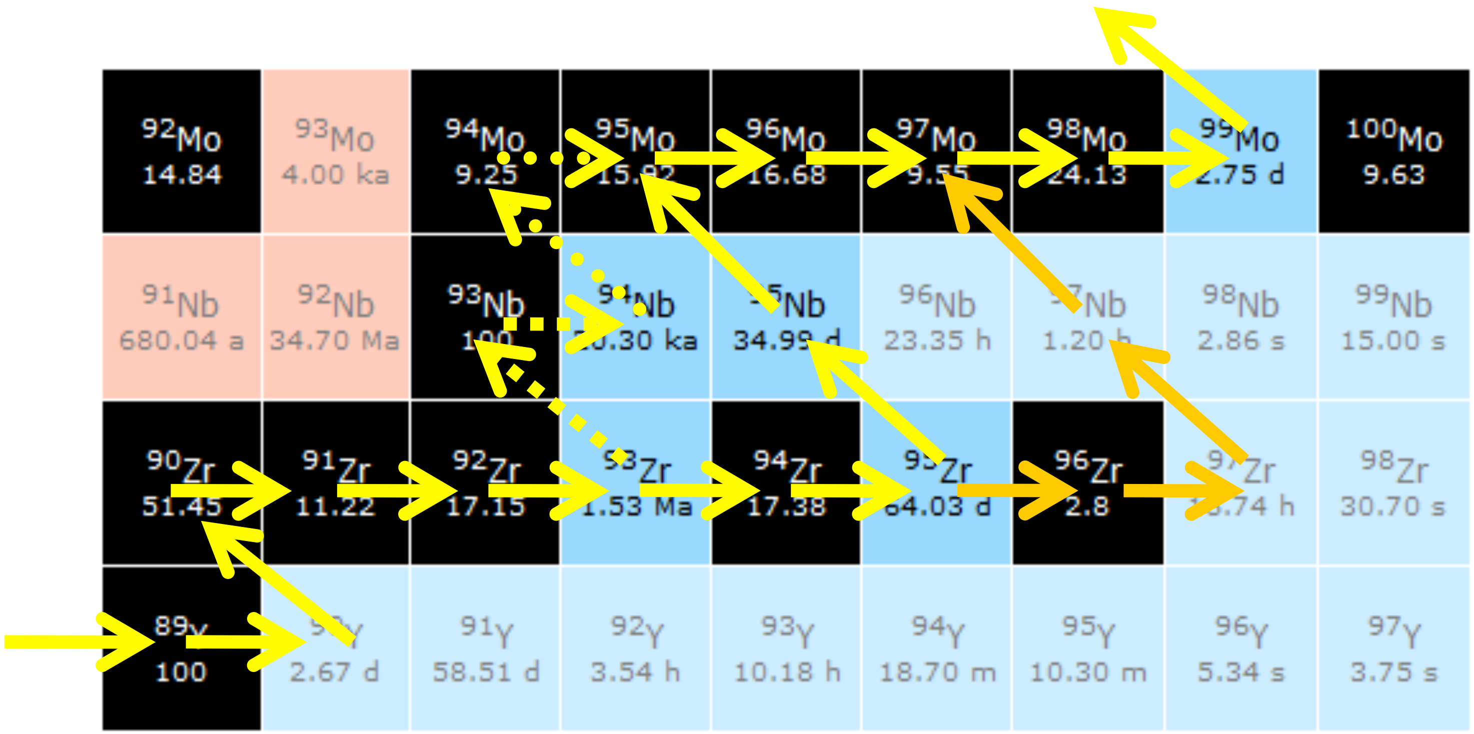

^{92}Mo 14.84
^{93}Mo 4.00 ka
^{94}Mo 9.25
^{96}Mo 16.68
^{98}Mo 24.13
^{100}Mo 9.63
^{91}Nb 680.04 a
^{92}Nb 34.70 Ma
^{96}Nb 23.35 h
^{98}Nb 2.86 s
^{99}Nb 15.00 s
^{91}Zr 11.22
^{92}Zr 17.15
^{94}Zr 17.38
^{96}Zr 2.8
^{98}Zr 30.70 s
^{89}Y 100
2.67 d
^{91}Y 58.51 d
^{92}Y 3.54 h
^{93}Y 10.18 h
^{94}Y 18.70 m
^{95}Y 10.30 m
^{96}Y 5.34 s
^{97}Y 3.75 s

Neutron in laboratory

Thermal reactors

almost monoenergetic neutron, very high flux

Monoenergetic neutron

Based on reaction (p,n) or (d,n)

d(d,n), t(p,n), ^{7}Li(p,n), ^{9}Be(p,n)

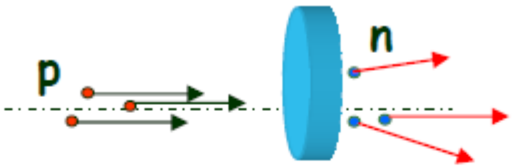

^{7}Li(p,n)^{7}Be

Time of Flight facilities

wide neutron energy spectrum

High energy resolution

Time of Flight facilities

Photoproduction (γ,n): Heavy metal targets are bombarded by electron beams of typical 20 -150 MeV. The resulting neutron spectra contains all energies from thermal to near the initial γ energy. ORELA, GELINA and RPI

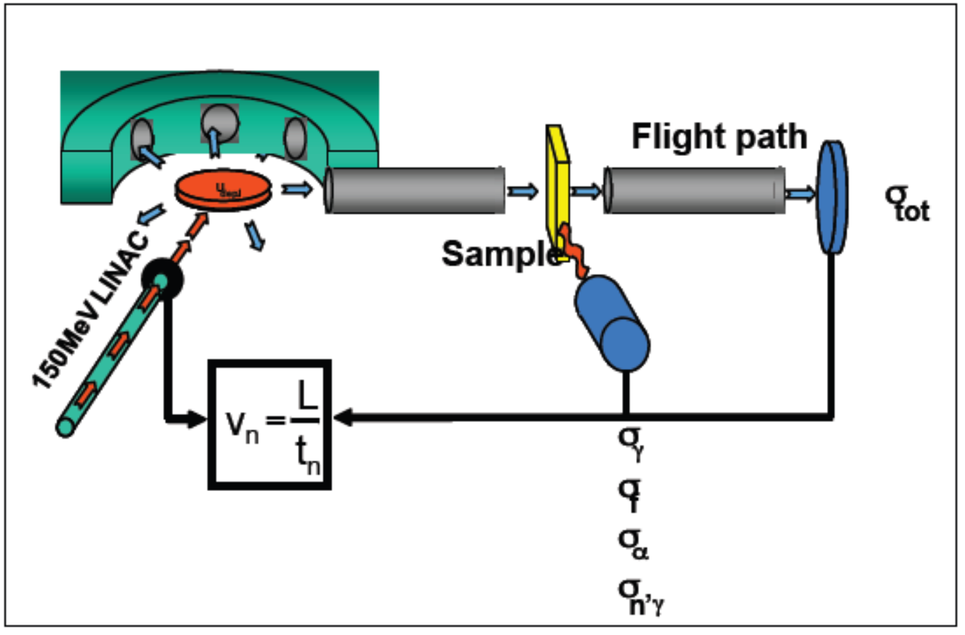

Time of Flight facilities

Spallation: neutron are are ejected from a heavy target due to the impact of charged particles as protons. It provides the most prolific source of fast neutrons.

n_TOF, LANCSE, ISIS

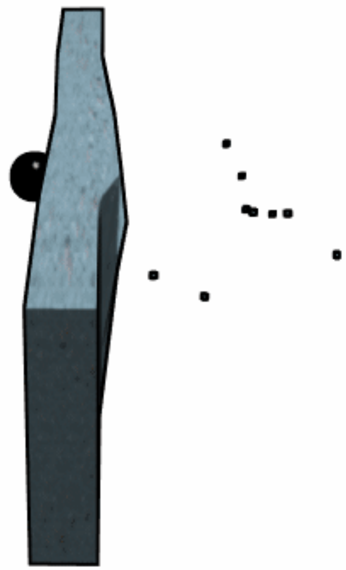

Time of Flight Technique

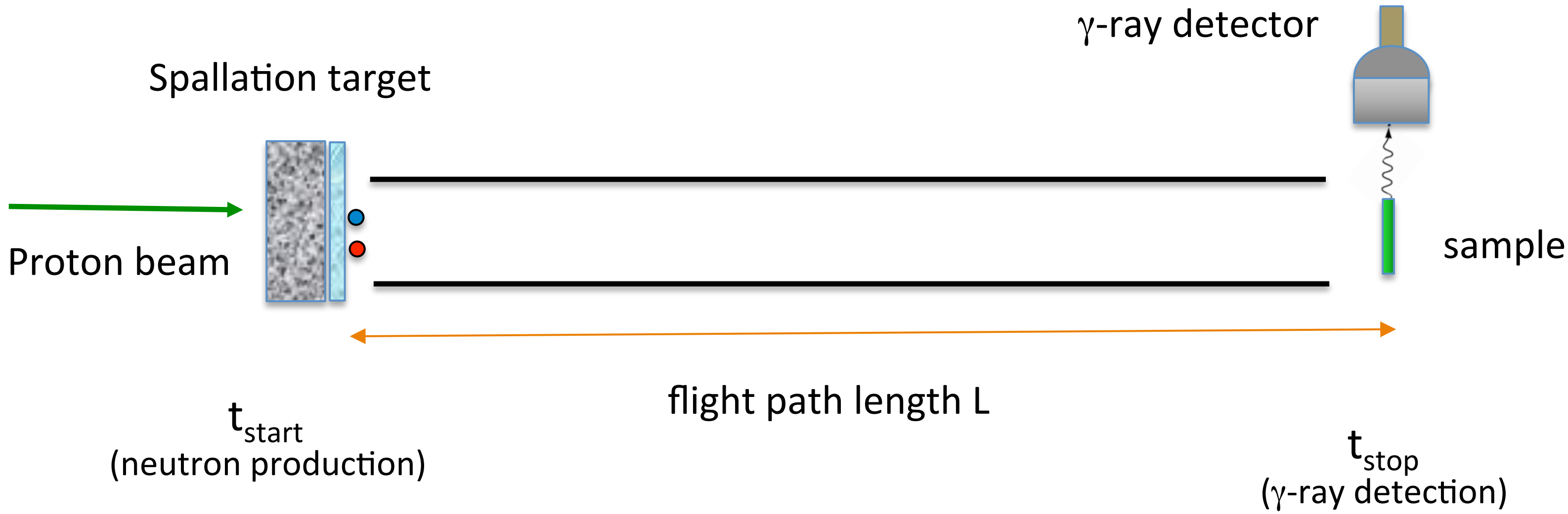

$$tof = t_{stop} - t_{star}$$

$$E_n = \left(\frac{72{,}2977 \cdot L}{tof} \right)^2$$

$$E_n = m_n c^2 \left(\frac{1}{\sqrt{1 - \frac{L^2}{tof^2 \cdot c^2}}} - 1 \right)$$

ToF Technique (Flux & Energy resolution)

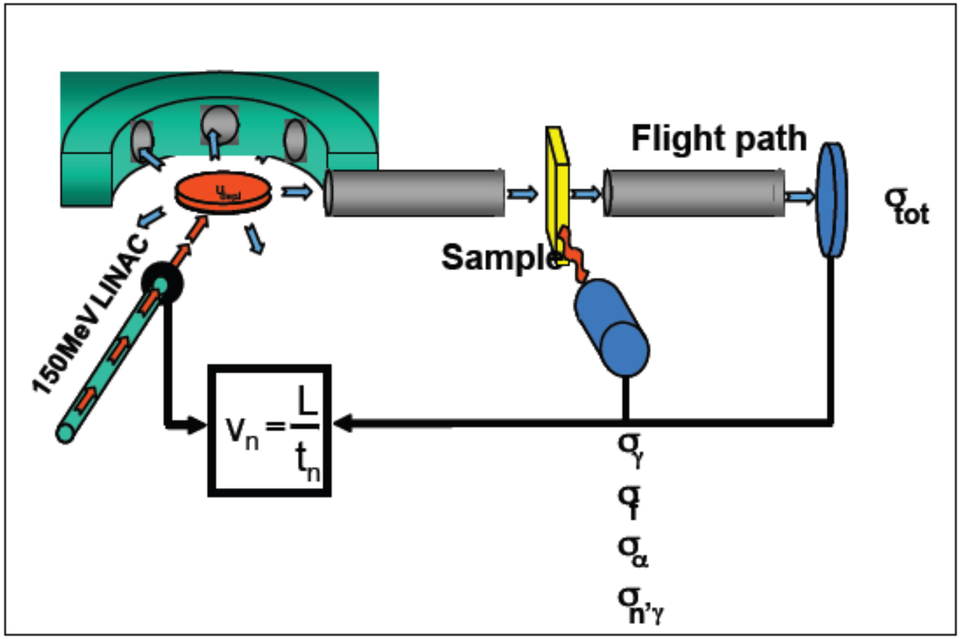

- **Velocity from TOF**

$$v_n = \frac{L}{t_n}$$

- **Resolution** $\Rightarrow L \nearrow$

$$\frac{\Delta v_n}{v_n} = \sqrt{\frac{\Delta t_n^2}{t_n^2} + \frac{\Delta L^2}{L^2}}$$

- **Neutron flux** $\Rightarrow L \searrow$

$$\varphi_n(L) \propto \frac{1}{L^2}$$

n_TOF facility at CERN

somewhere around here

The CERN n_TOF Facility

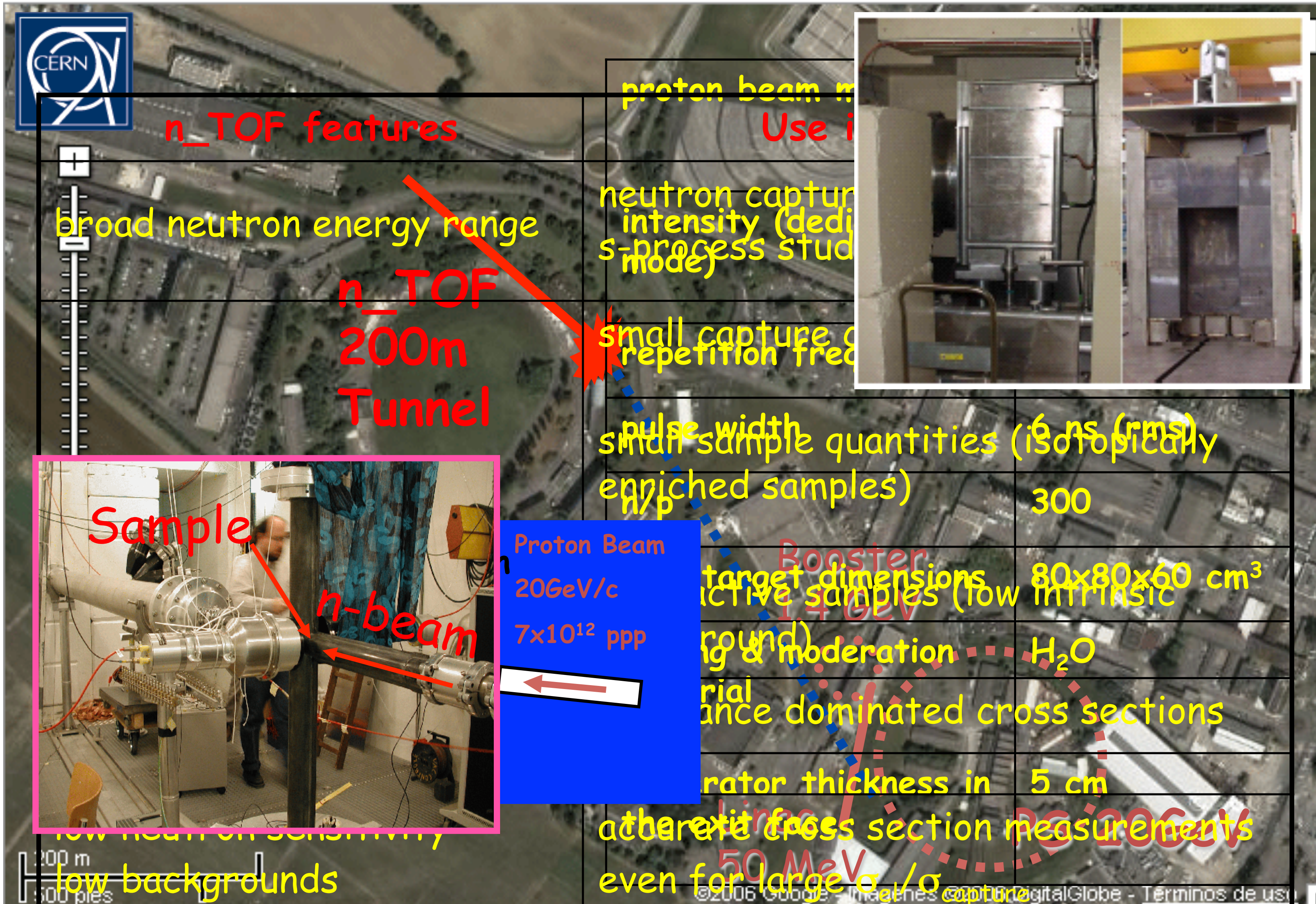

GELINA Facility

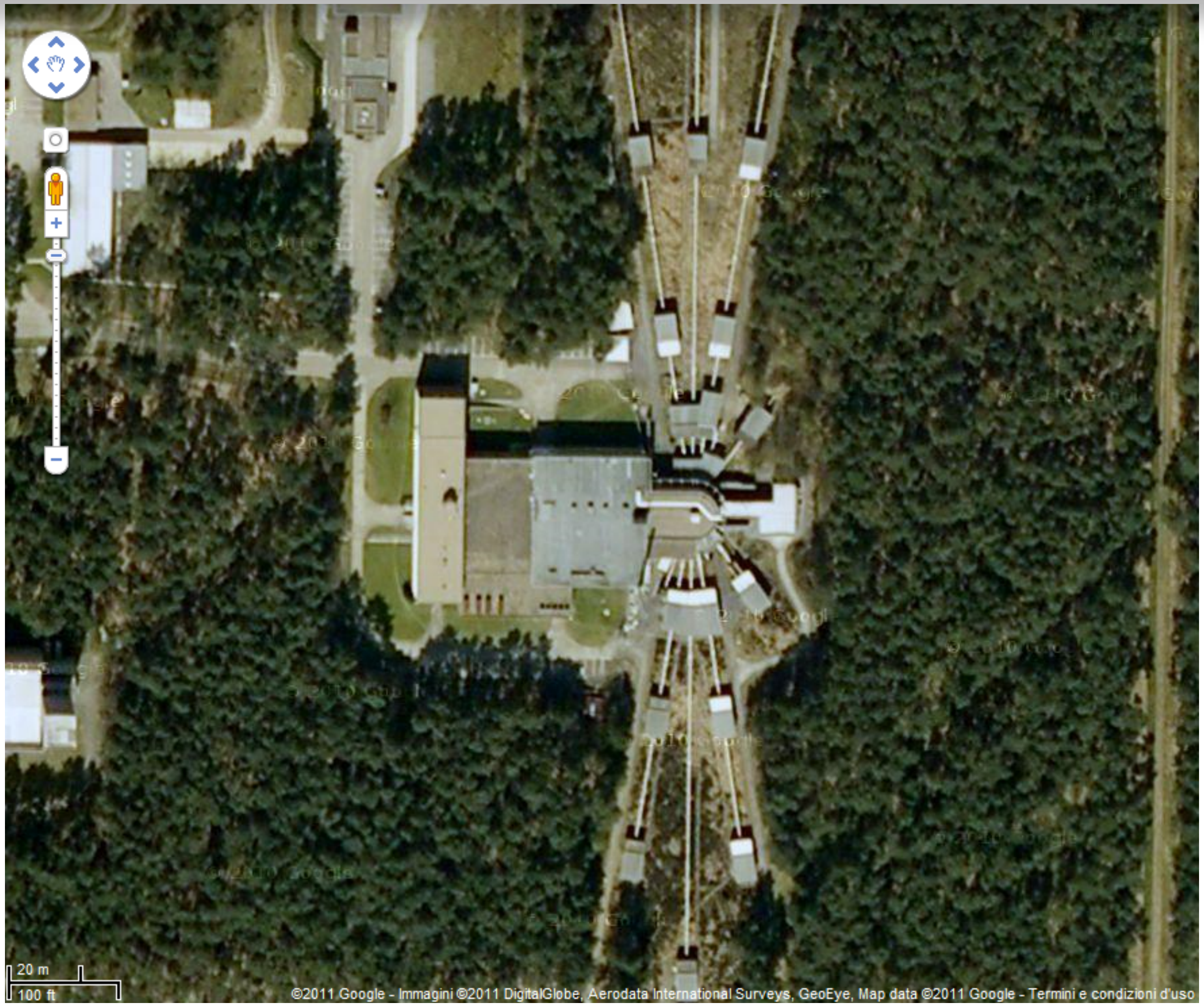

GELINA Facility

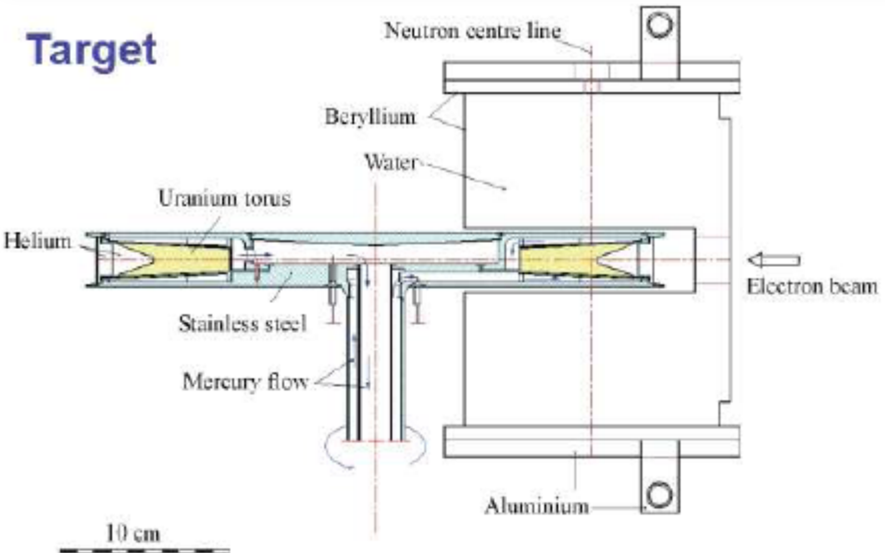

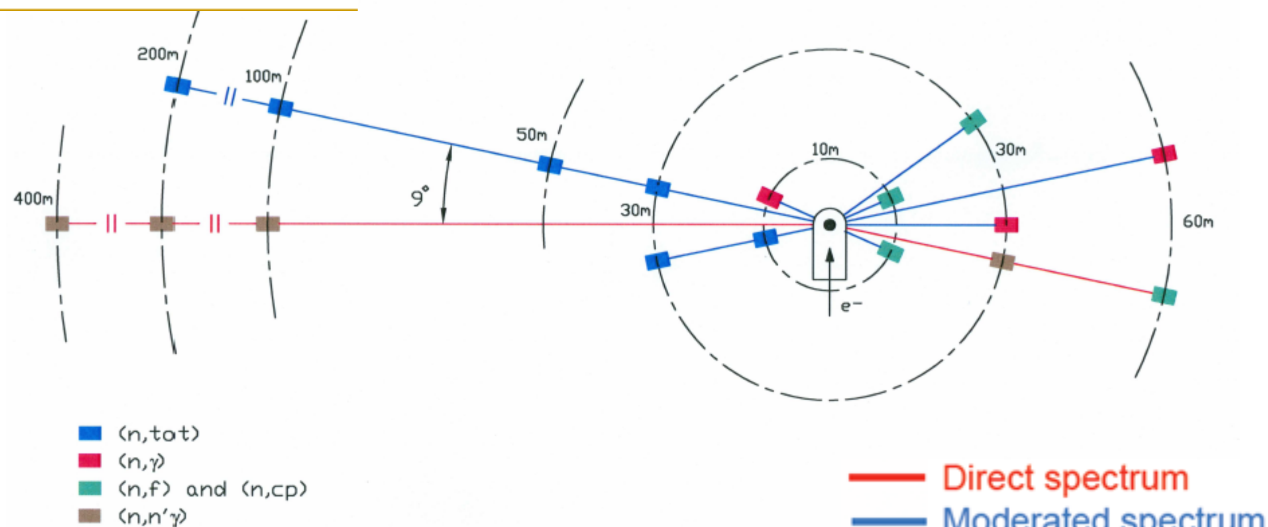

Flux

Integrated neutron flux

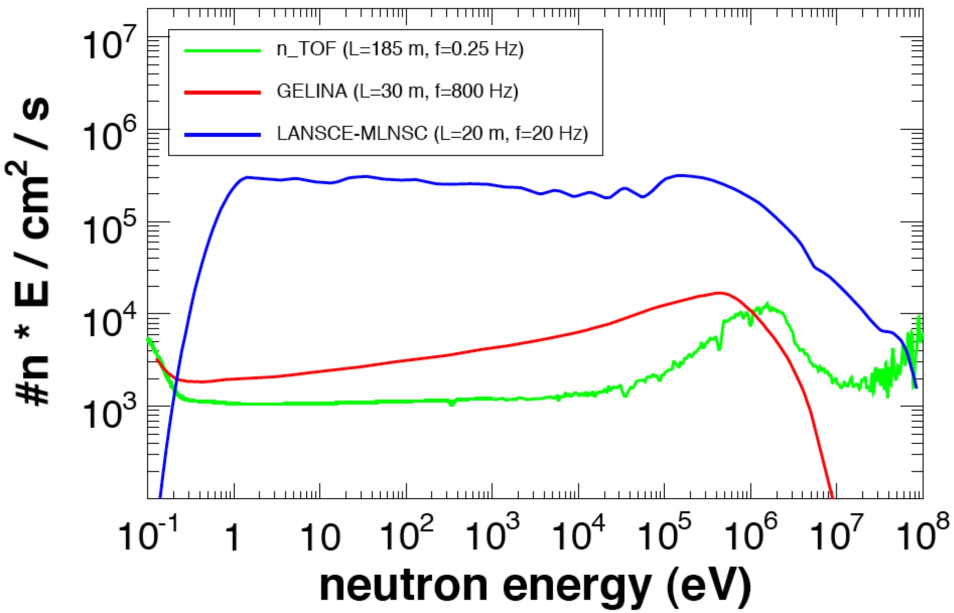

Istantaneous neutron fllux

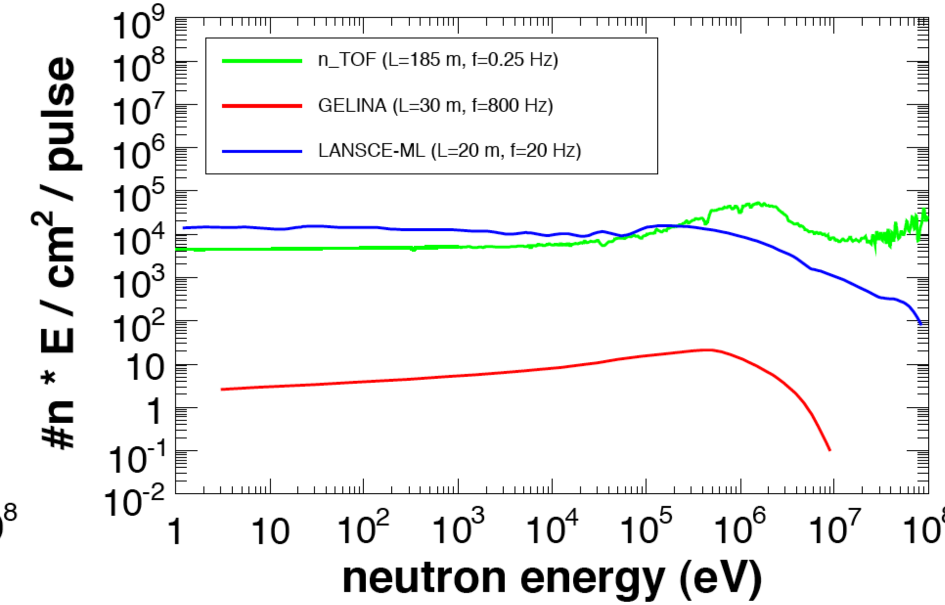

Resolution

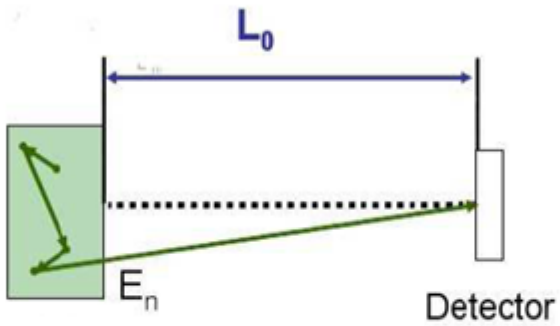

L = L0 + Lm

$$L = L(E_n) = L_0 + \Delta L(E_n)$$

$$E_n = \frac{1}{2} m_n v^2 = \frac{1}{2} m_n \left(\frac{L}{t}\right)^2$$

$$E_n = \frac{1}{2} m_n v^2 = \left(\frac{72.2977\, L_0}{t + t_{0ff}}\right)^2$$

n_TOF GELINA Resolution

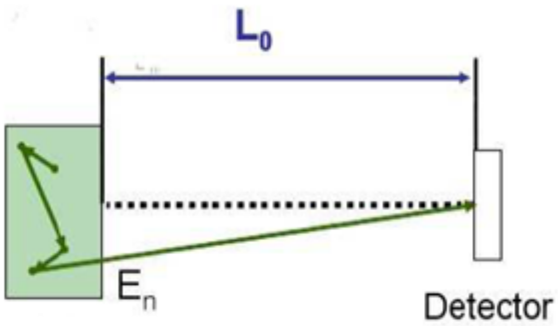

$L = L_0 + L_m$

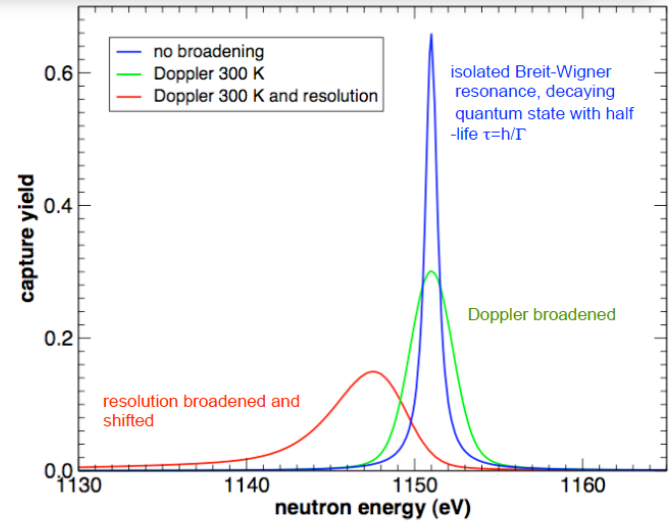

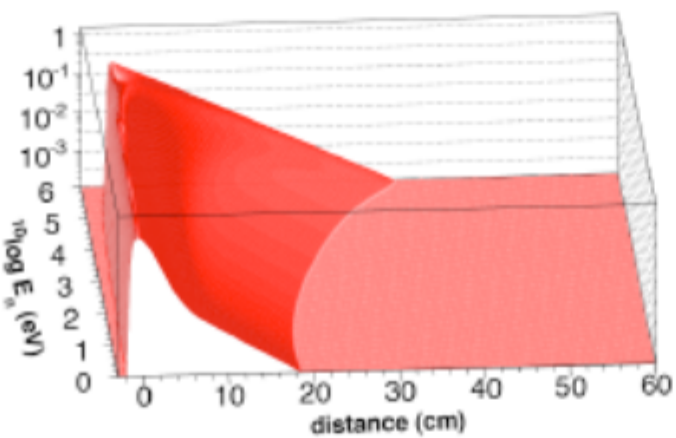

GELINA

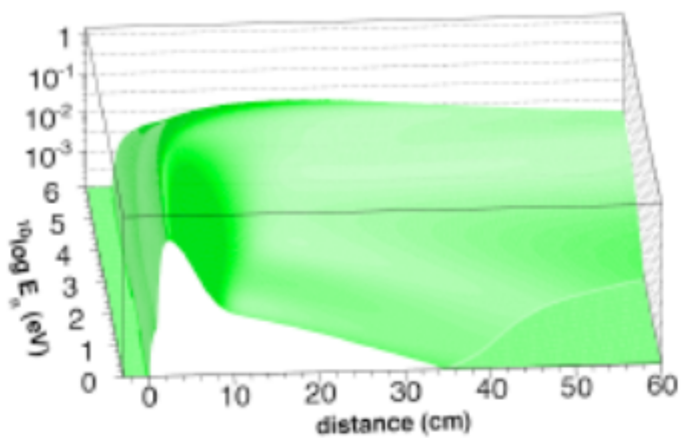

n_TOF

Neutron Capture

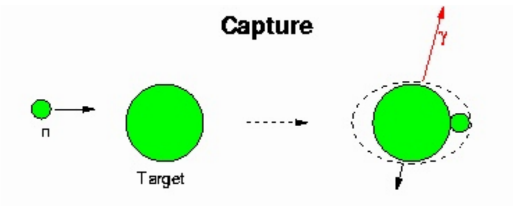

$$E^* = S_n + \frac{A}{A+1} E_n$$

$$E^* = \sum_j E_j^\gamma$$

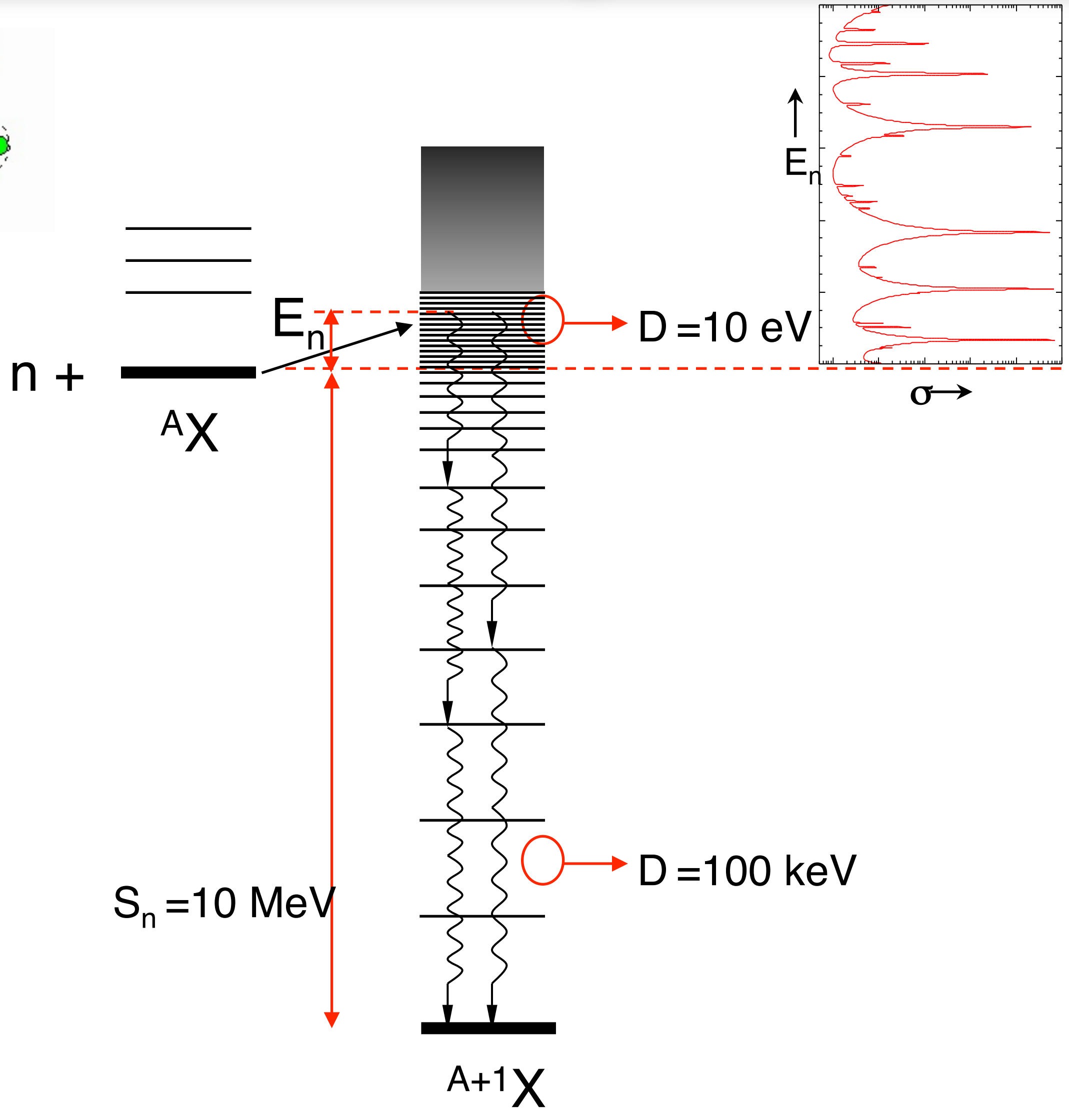

Neutron Capture: Cross Section

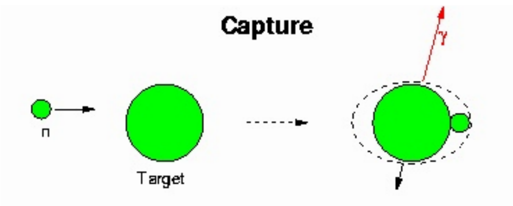

$$E^{*} = S_n + \frac{A}{A+1} E_n$$

$$\sigma_{c^*}(E_n) = g\frac{\pi}{k_n^2}\frac{\Gamma_n \Gamma}{(E_n - E_0)^2 + \left(\frac{\Gamma}{2}\right)^2}$$

g spin factor

k_n neutron wave number

$\Gamma = \Gamma_n + \Gamma_g + \Gamma_f + \ldots$

Γ total width

Γ_n neutron scattering width

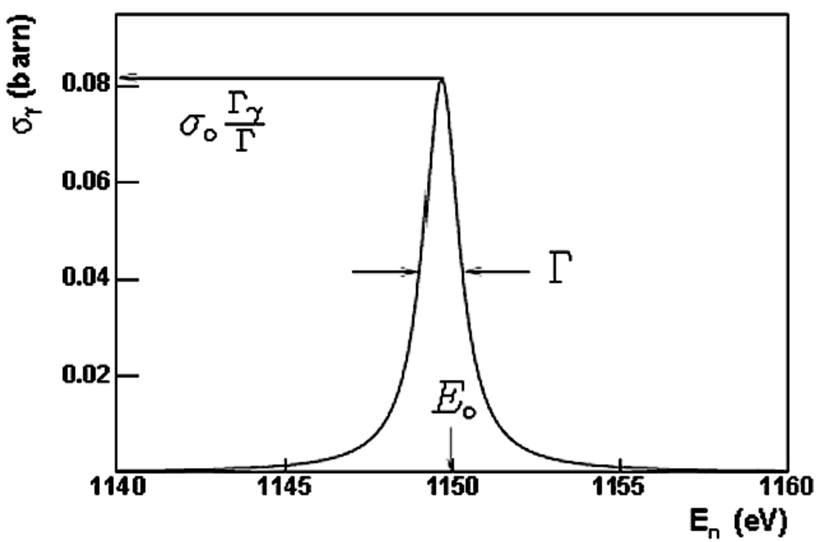

$$\sigma_0 = \frac{4\pi}{k_n^2} g \frac{\Gamma_n}{\Gamma}$$

Total radiative area:

$$A_r = \frac{2\pi^2}{k_0^2} g \frac{\Gamma_n \Gamma_\gamma}{\Gamma}$$

Neutron Capture: Resonances

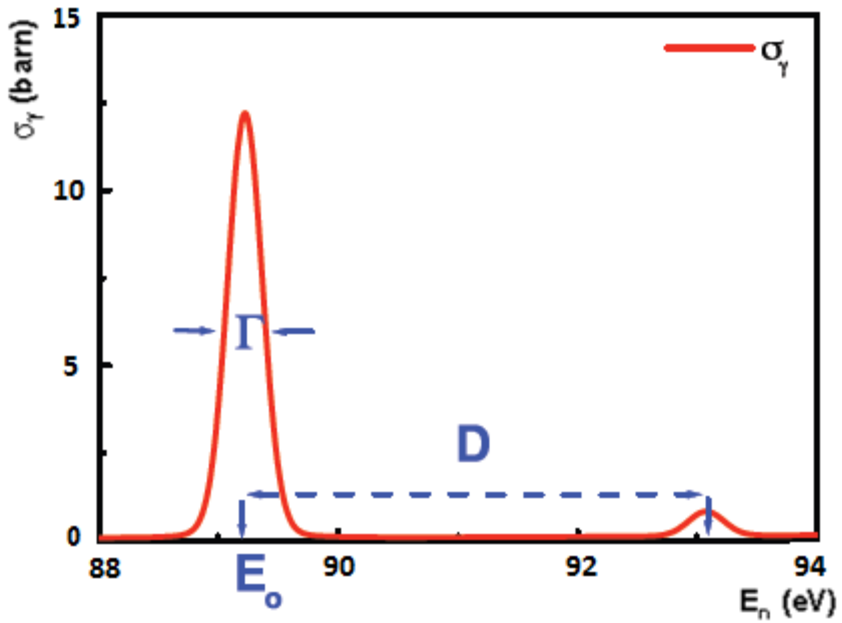

Resonance Region: Γ < D

Resolved Resonance Region (RRR): Detection resolution < D

Unresolved Resonance Region (URR): Detection resolution > D

Neutron Capture Gamma-Ray Detection

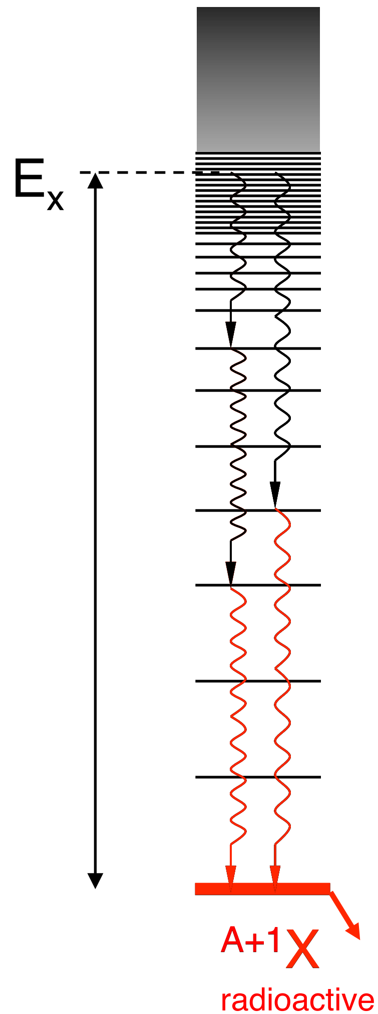

- **Activation**
  - cross sections integrated over known neutron spectrum
  - applicable to some nuclei only
  - no time of flight

- **Level population spectroscopy**
  - applicable to some nuclei only
  - feasible with HPGe detectors,

- **Total energy detection**
  - $\varepsilon_c \sim E_x$, requires weighting function
  - neutron insensitive detector

  C_6D_6 detector used at GELINA and n_TOF

- **Total absorption detection**
  - requires $\Omega = 4\pi$, efficiency 100%
  - capture/fission discrimination possible

  BaF_2 detector used at n_TOF

(n,γ) Total energy detection

Improvements in the Experimental Setup & Data Analysis

- Lowest neutron sensitivity ➡ No neutron background corrections !

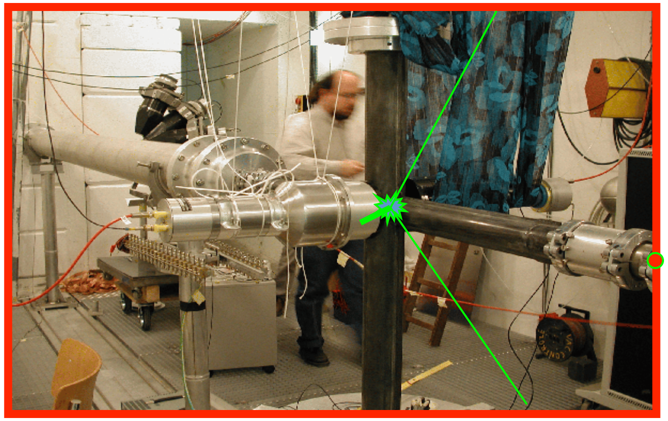

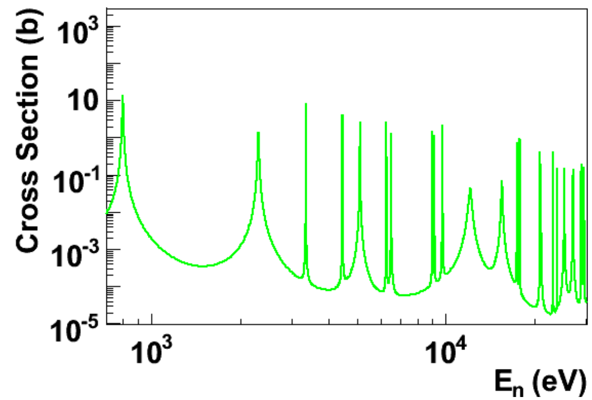

(n,γ)

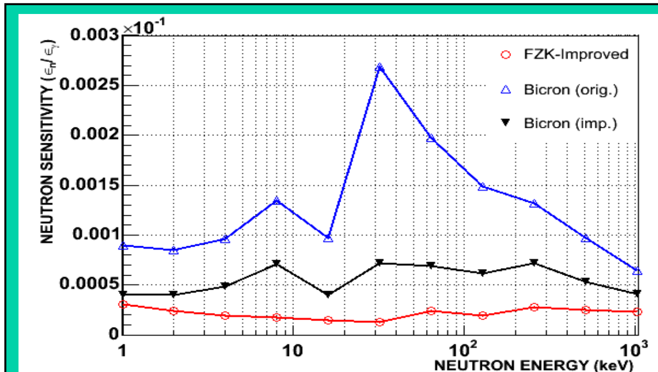

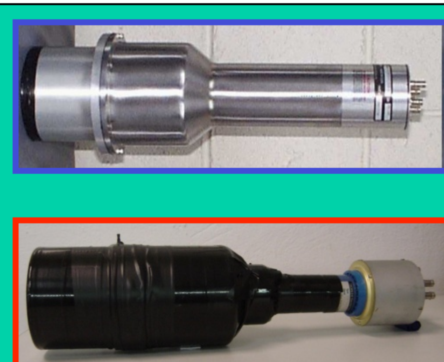

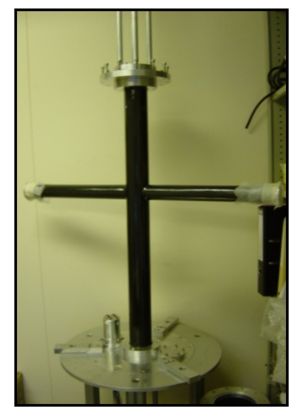

(n,γ) Total energy detection

Improvements in the Experimental Setup & Data Analysis

- Lowest neutron sensitivity ➡ No neutron background corrections !

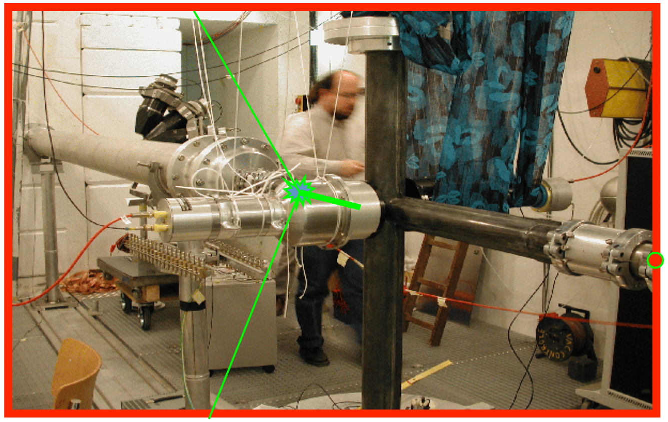

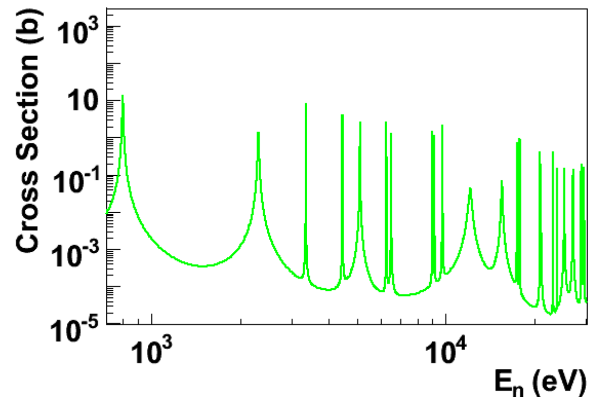

(n,n)

(n,γ)

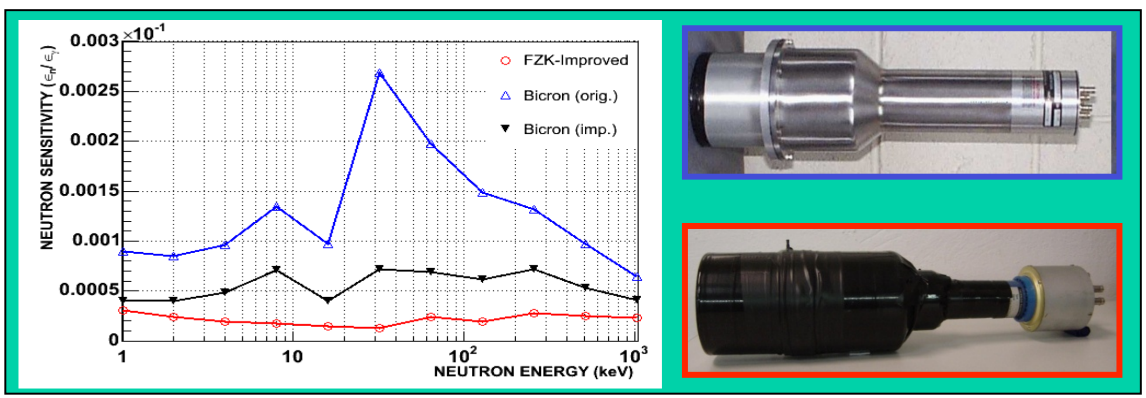

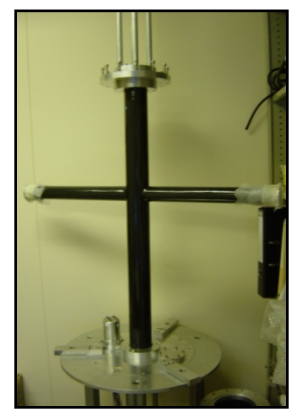

Experimental details: Yield

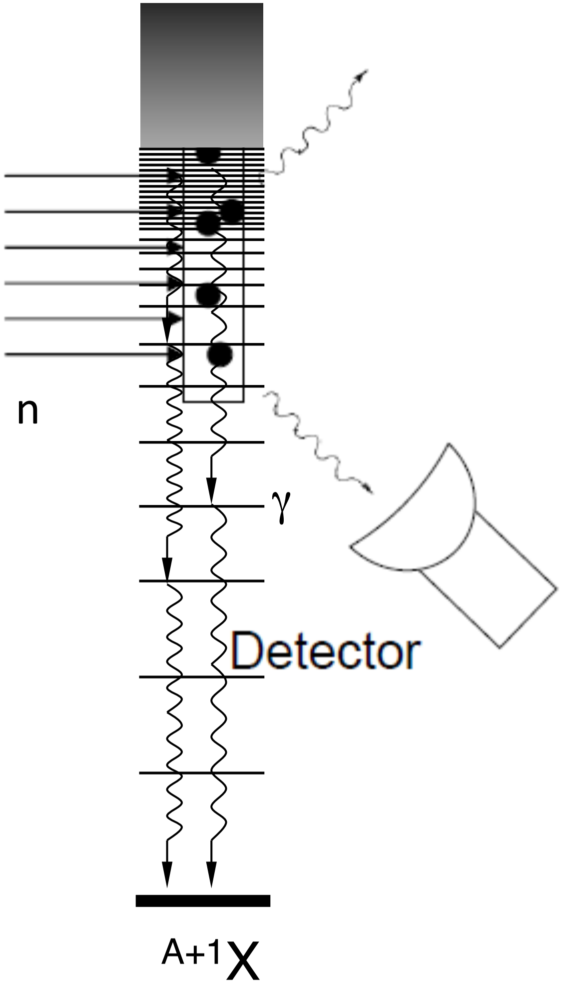

Yield: The fraction of incident neutrons undergoing a (n,γ) reaction in the sample

$$Y_{exp} = \frac{N(E_n, E_{dep})}{N_n(E_n) \times \varepsilon(E_n, E_{dep})}$$

The relation between capture Yield and cross section is given by:

$$Y = (1 - e^{-n\sigma_{tot}})\frac{\sigma_\gamma}{\sigma_{tot}}$$

Experimental details: PHWT

Accuracy of the Pulse Height Weighting Technique? (used to count properly capture cascades)

$$\sum_i W_i R_{ij} = E_j$$

Use of detailed MC simulations of detector response with the full setup

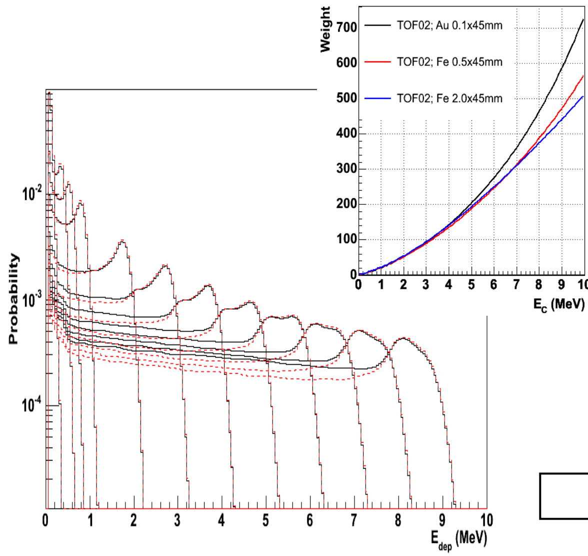

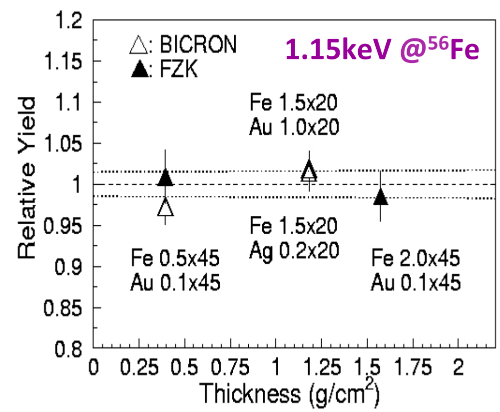

+

Use of the nuclear statistical model to make systematic corrections

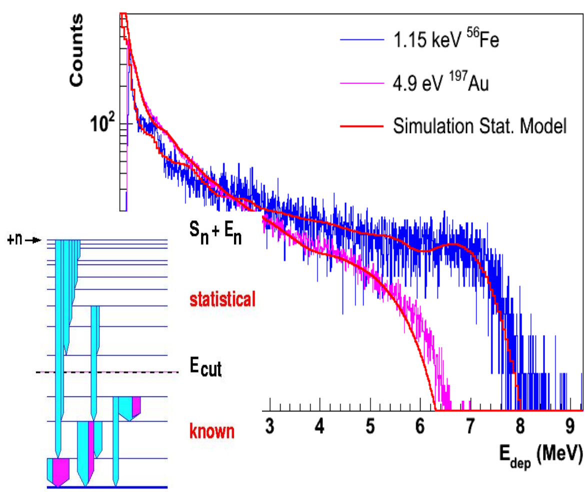

… accuracy < 2%

Experimental details: Sample

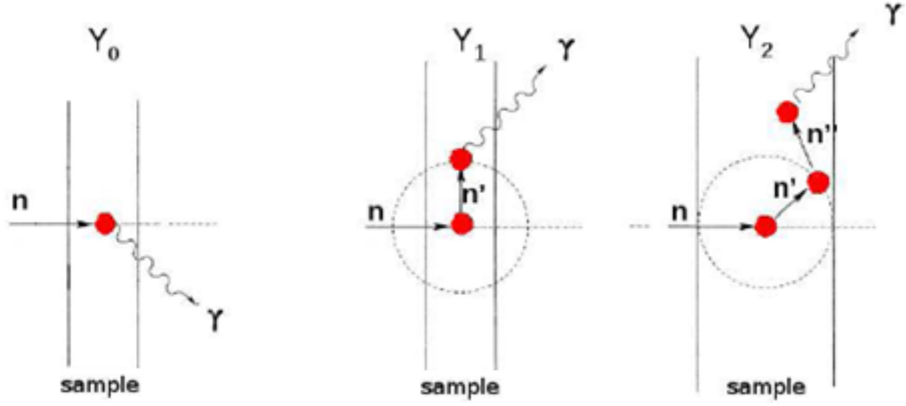

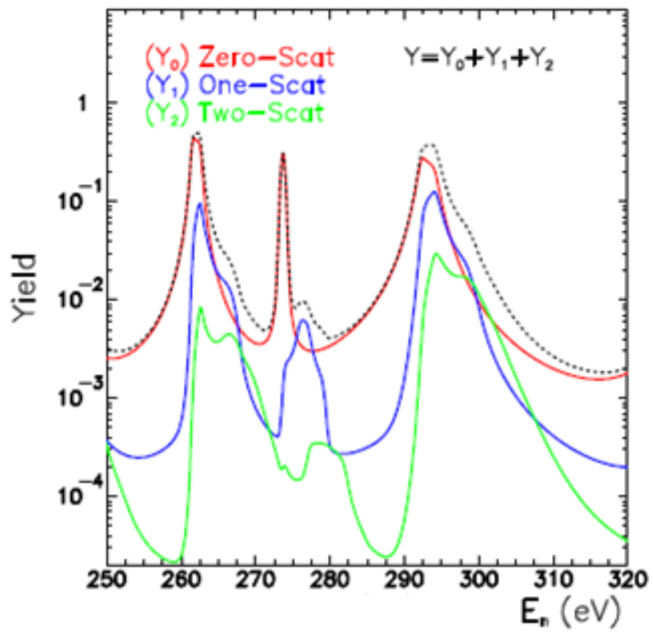

Experimental details: Area analysis

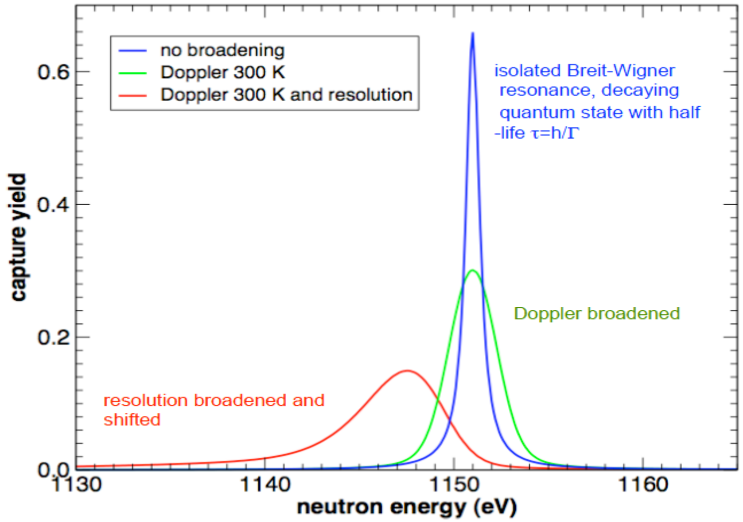

Due to the instrumental limitations and Doppler effect the effective observable is: The area of a resonance.

The area below a resonance is independent of the experimental resolution and Doppler effect

$$A_{tot} = \int (1 - e^{-n\sigma_{tot}}) dE$$

$$A_{\gamma} = \int (1 - e^{-n\sigma_{tot}}) \frac{\sigma_{\gamma}}{\sigma_{tot}} dE$$

Experimental details: Area analysis

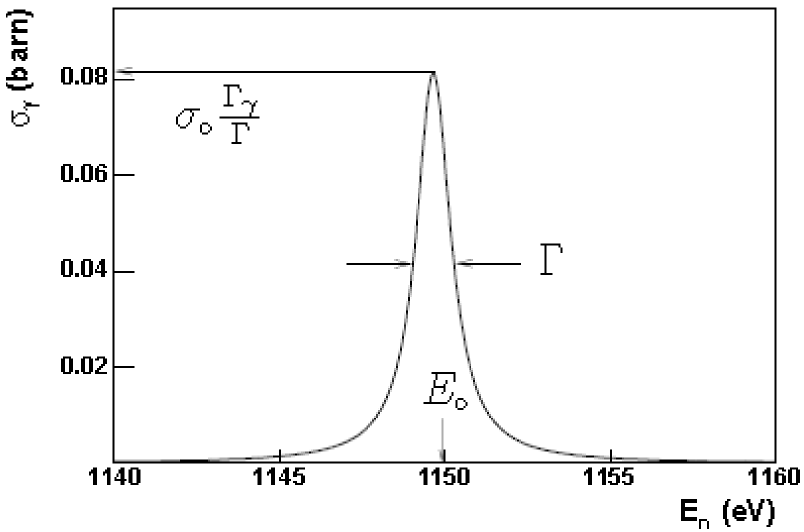

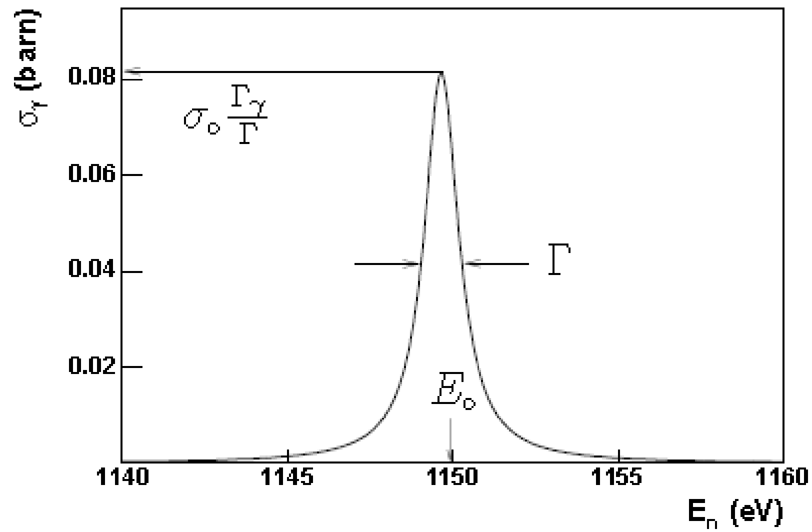

$$A_\gamma(thin) = \frac{1}{2}\pi n \sigma_0 \Gamma_n = 2n\pi^2 ƛ^2 g \frac{\Gamma_n \Gamma_\gamma}{\Gamma}$$

$$A_{tot}(thin) = \frac{1}{2}\pi n \sigma_0 \Gamma = 2n\pi^2 ƛ^2 g \Gamma_n$$

$$A_{tot}(thick) = \sqrt{\pi n \sigma_0 \Gamma} = 2\pi ƛ \sqrt{n g \Gamma_n \Gamma}$$

$$A_\gamma = 2n\pi^2 K ƛ$$

$$K = g\frac{\Gamma_n \Gamma_\gamma}{\Gamma}$$

Experimental details: Normalization

$$Y_{exp} = \frac{N(E_n, E_{dep})}{N_n(E_n) \times \varepsilon(E_n, E_{dep})}$$

^{197}Au

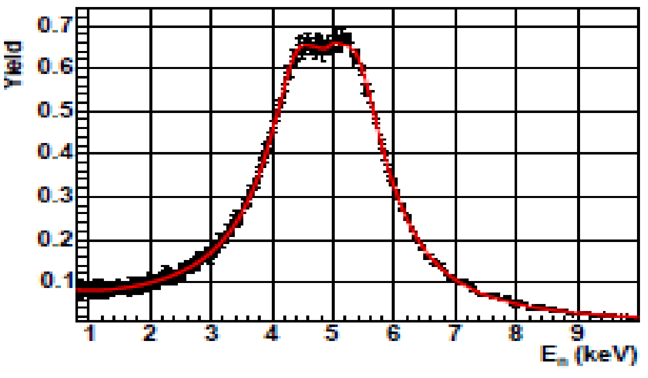

$$Y_{ref}^{exp}(E_n) = \frac{N_{ref}^{w}(E_n)}{N_n(E_n) \times (S_n^{ref} + E_n)}$$

$$Y_{ref}^{exp}(E_n) = A Y_{ref}^{th}(E_n) + B \rightarrow f^{Sat} = \frac{1}{A}$$

Maxwellian Averaged Cross Sections:MACS

Neutrons produced in the stars are quickly thermalised ➡ **M-B distribution**

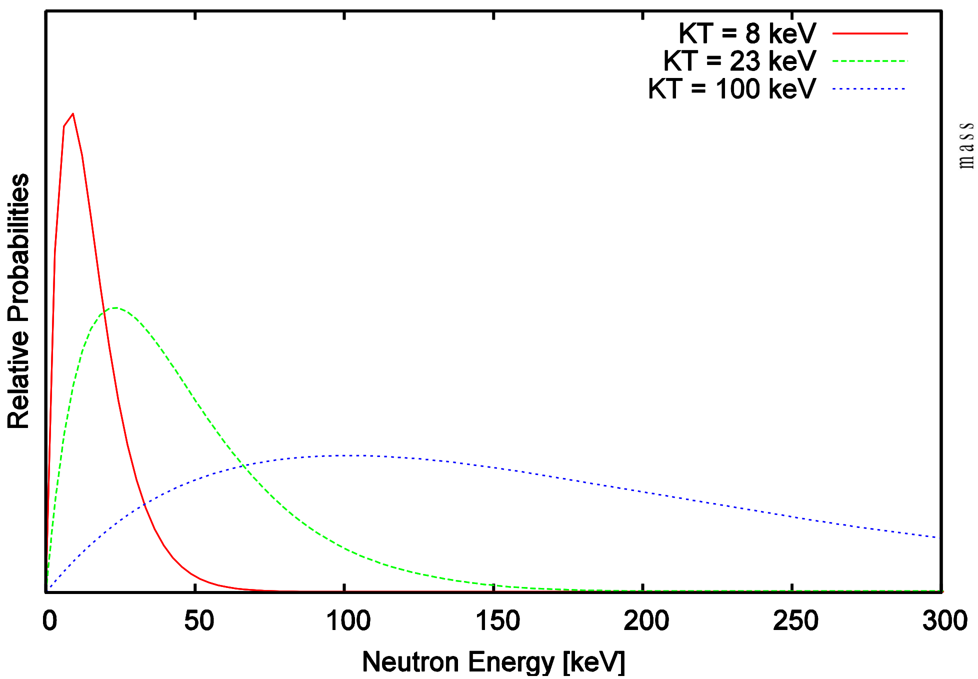

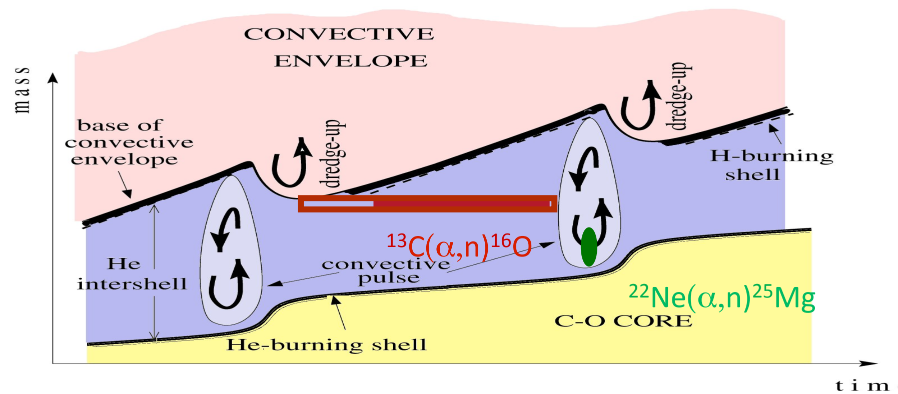

Maxwellian Averaged Cross Sections:MACS

Neutrons produced in the stars are quickly thermalised ⇨ **M-B distribution**

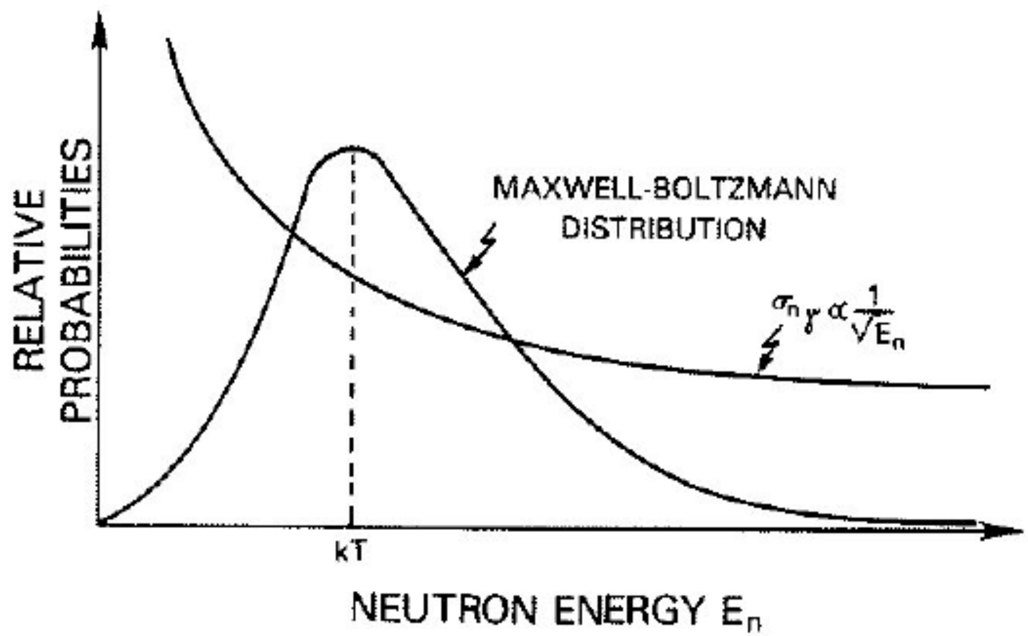

Data analysis: Main steps

- Energy Calibration (^{137}Cs,^{60}Co,Pu/C)
- Noise rejection by suitable choice of cuts and threshold
- Efficiency correction → PHWT
- Background estimation
- Flux normalization

The Zr case

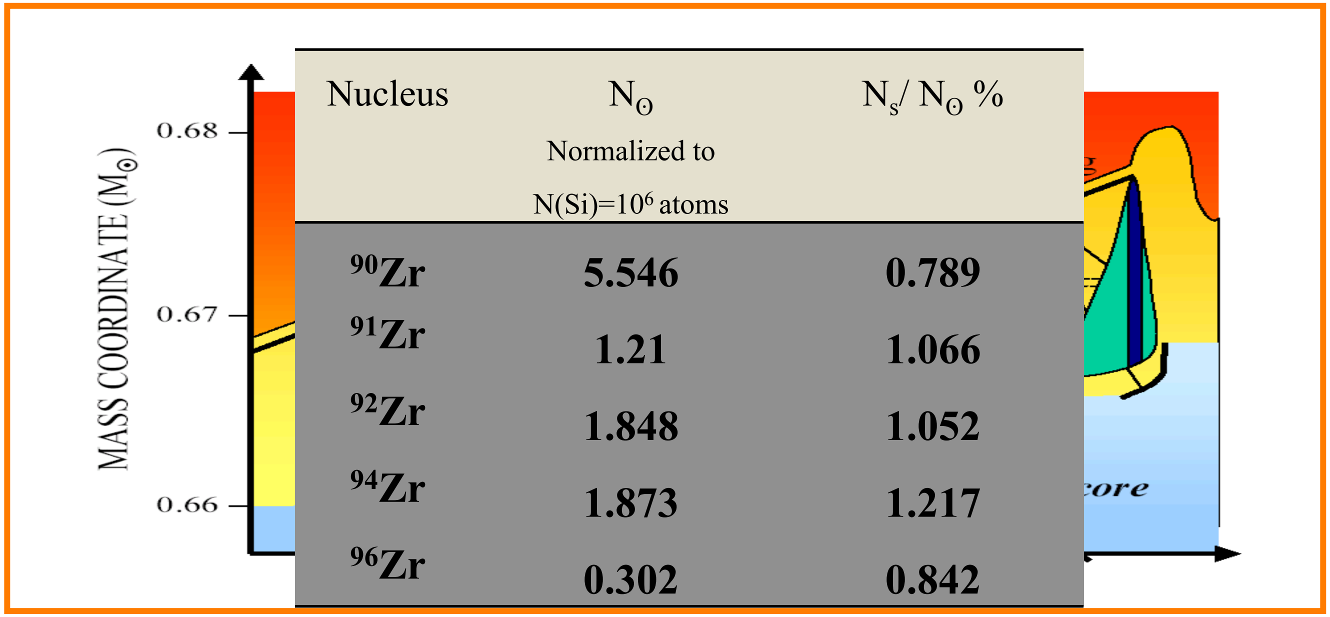

Nucleus	$N_\odot$ Normalized to N(Si)=10^6 atoms	$N_s / N_\odot$ %
^{90}Zr	5.546	0.789
^{91}Zr	1.21	1.066
^{92}Zr	1.848	1.052
^{94}Zr	1.873	1.217
^{96}Zr	0.302	0.842

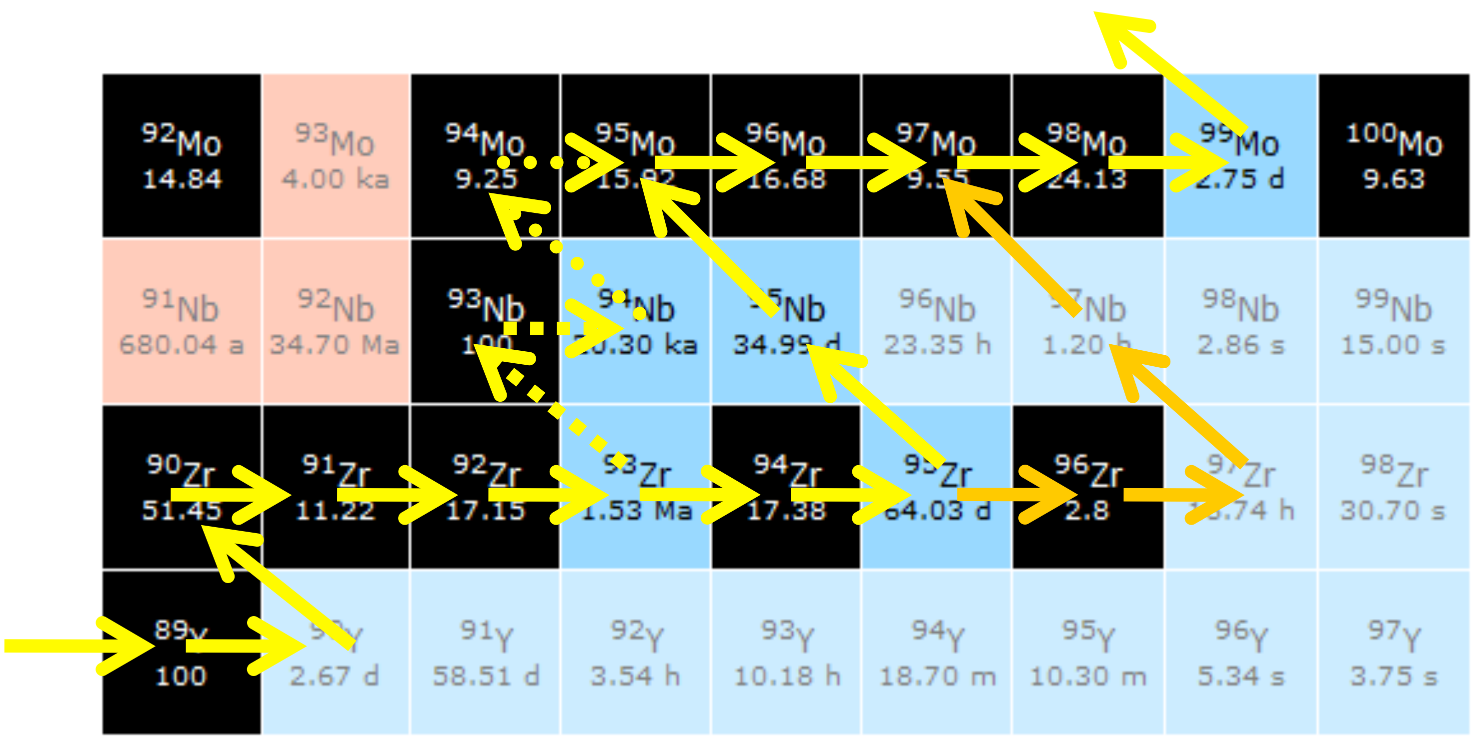

Zr in SiC grains

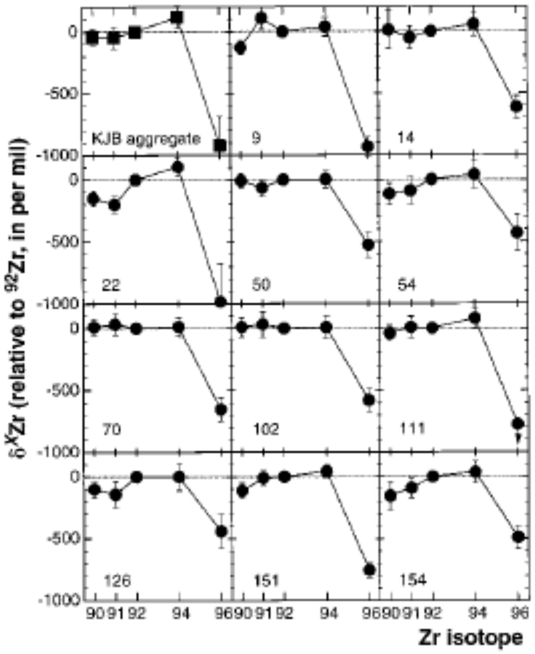

MACS: Experimental energy ranges

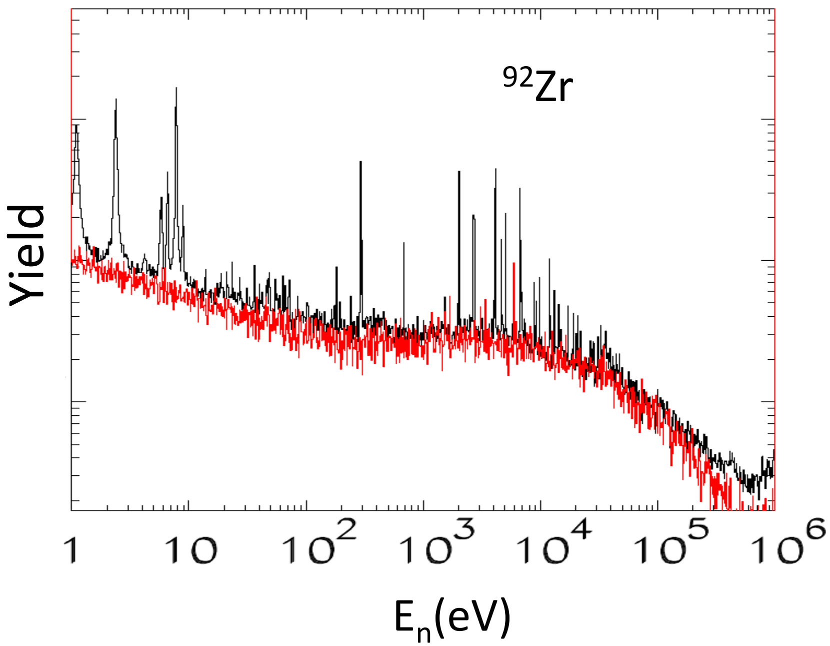

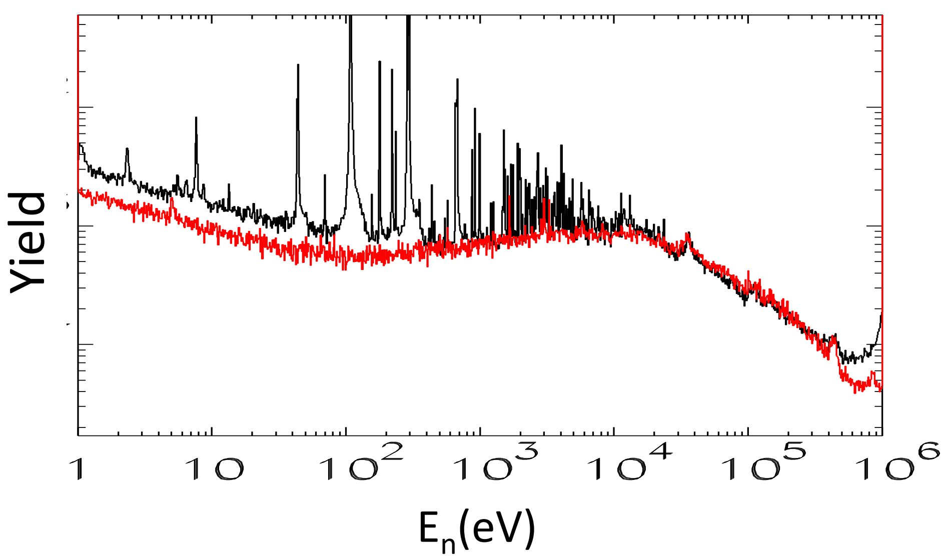

	Energy range investigated(KeV) n_TOF
^{90}Zr	0.01 - 66
^{91}Zr	0.01 - 26
^{92}Zr	0.01 – 40
^{93}Zr	0.01 – 7
^{94}Zr	0.01 – 74
^{96}Zr	0.01 – 42

The n_TOF data have to be complemented with the library Jendl 3.3 and ENDF IV

MACS:@ 30 keV

MACS in mbarn

Isotope	KaDoNiS	N_TOF	MOST
^{90}Zr	21 ± 2	19.3 ± 0.9	
^{91}Zr	60 ± 8	63 ± 4	
^{92}Zr	34 ± 6	38 ± 3	
^{93}Zr	95 ± 10	**95.± 5**	
^{94}Zr	26 ± 1	30.5 ± 2	
^{95}Zr	79	**20.9 ± 0.9**	24.2
^{96}Zr	10.7 ± 0.5	8.9 ± 0.5	

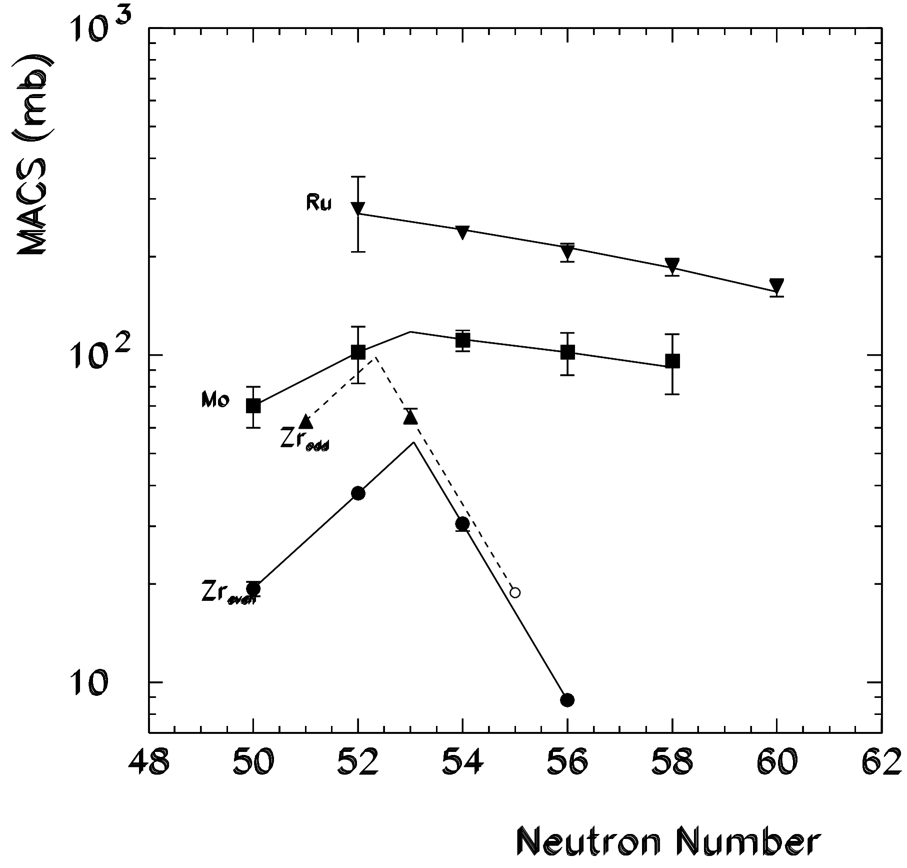

Astrophysical implication: Abundances

Nucleus	$N_{\odot}$ Normalized to $N(Si)=10^6$ atoms	$N_s/N_{\odot}$ % Old MACS	$N_s/N_{\odot}$ % MACS from this work
^{90}Zr	5.546	0.789	0.844
^{91}Zr	1.21	1.066	1.024
^{92}Zr	1.848	1.052	0.981
^{94}Zr	1.873	1.217	1.152
^{96}Zr	0.302	0.842	0.321

Ages

- Cosmological way
  based on the Hubble time definition ("expansion age")

- Astronomical way
  based on observations of globular clusters

- Nuclear way
  based on abundances & decay properties of long-lived radioactive species

The nuclear way

Traditional nuclear clocks are those based on:

- $^{235}U/^{238}U$
- $^{232}Th/^{238}U$
- $^{187}Os/^{187}Re$
- Th/Eu, Th/X or Th/U abundances in low-Z stars

Os measurements

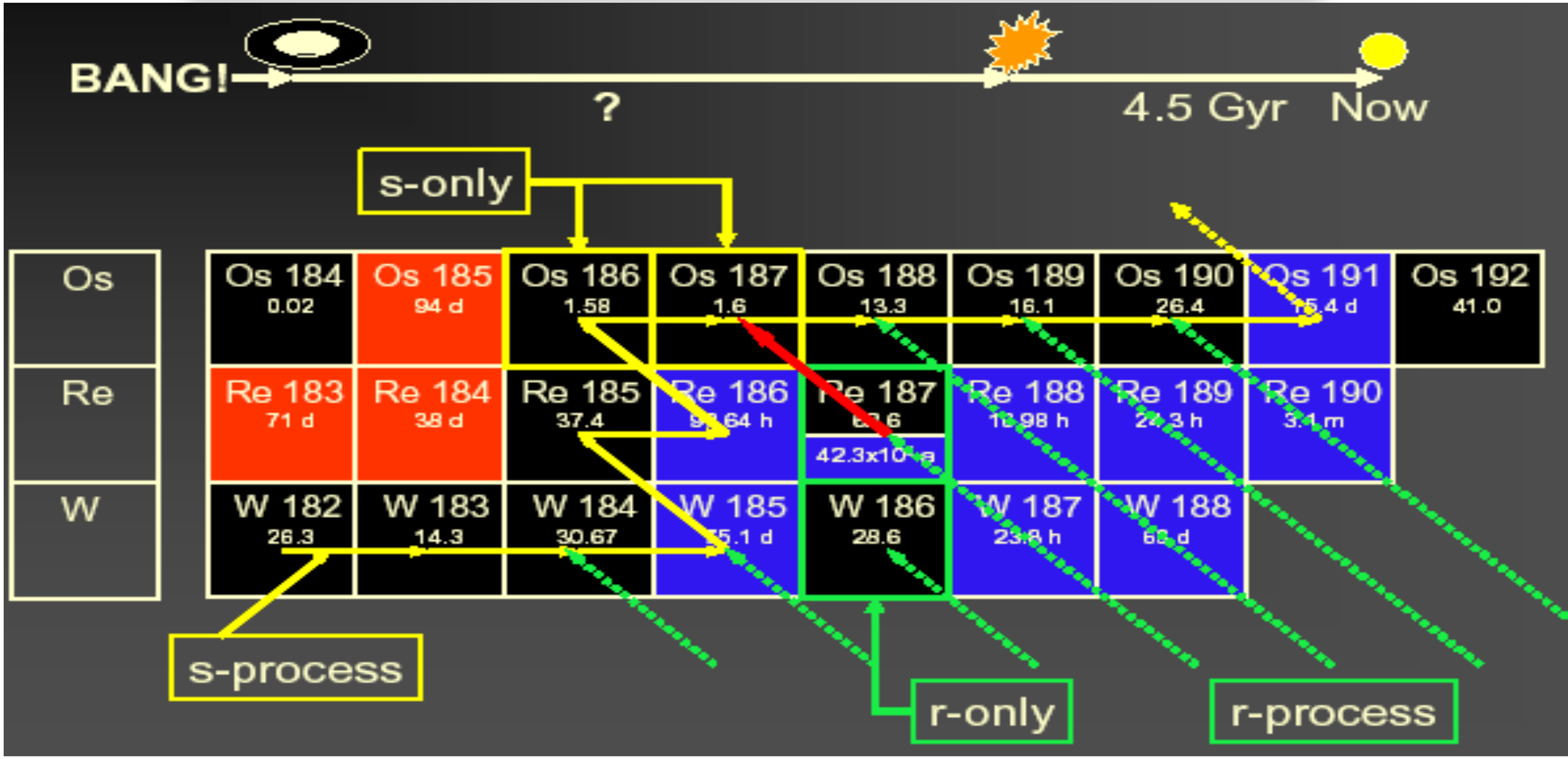

- Long β-decay half-life of ^{187}Re s-only ^{186}Os and ^{187}Os

Os: results

MACS-30	
BrB81	438 ± 30 mb
WiM82	418 ± 16 mb
n_TOF	384 ± 17 mb

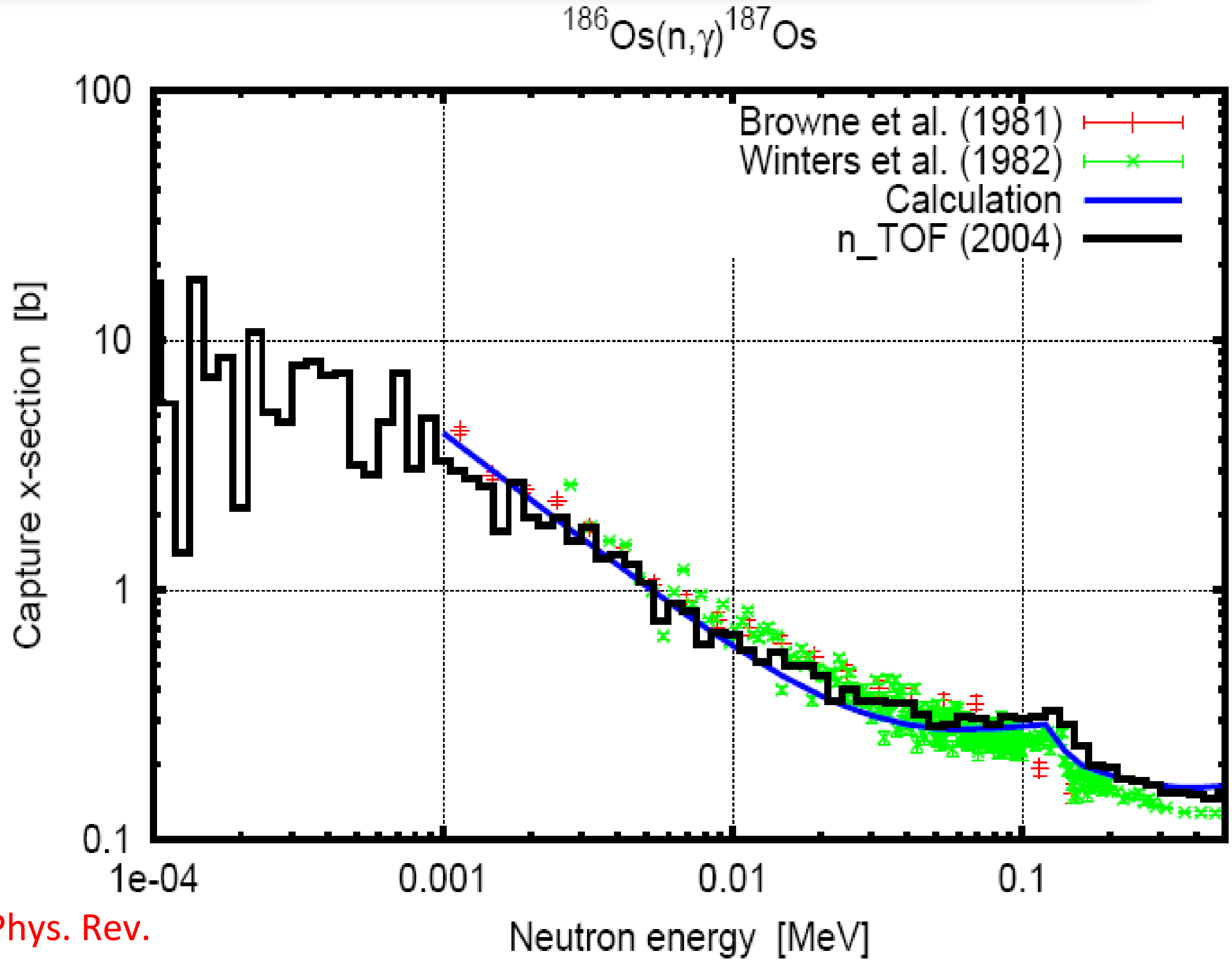

M. Mosconi et al.,Phys. Rev. C

Os: results

MACS-30	
BrB81	919 ± 28 mb
WiM82	874 ± 28 mb
n_TOF	940 ± 18 mb

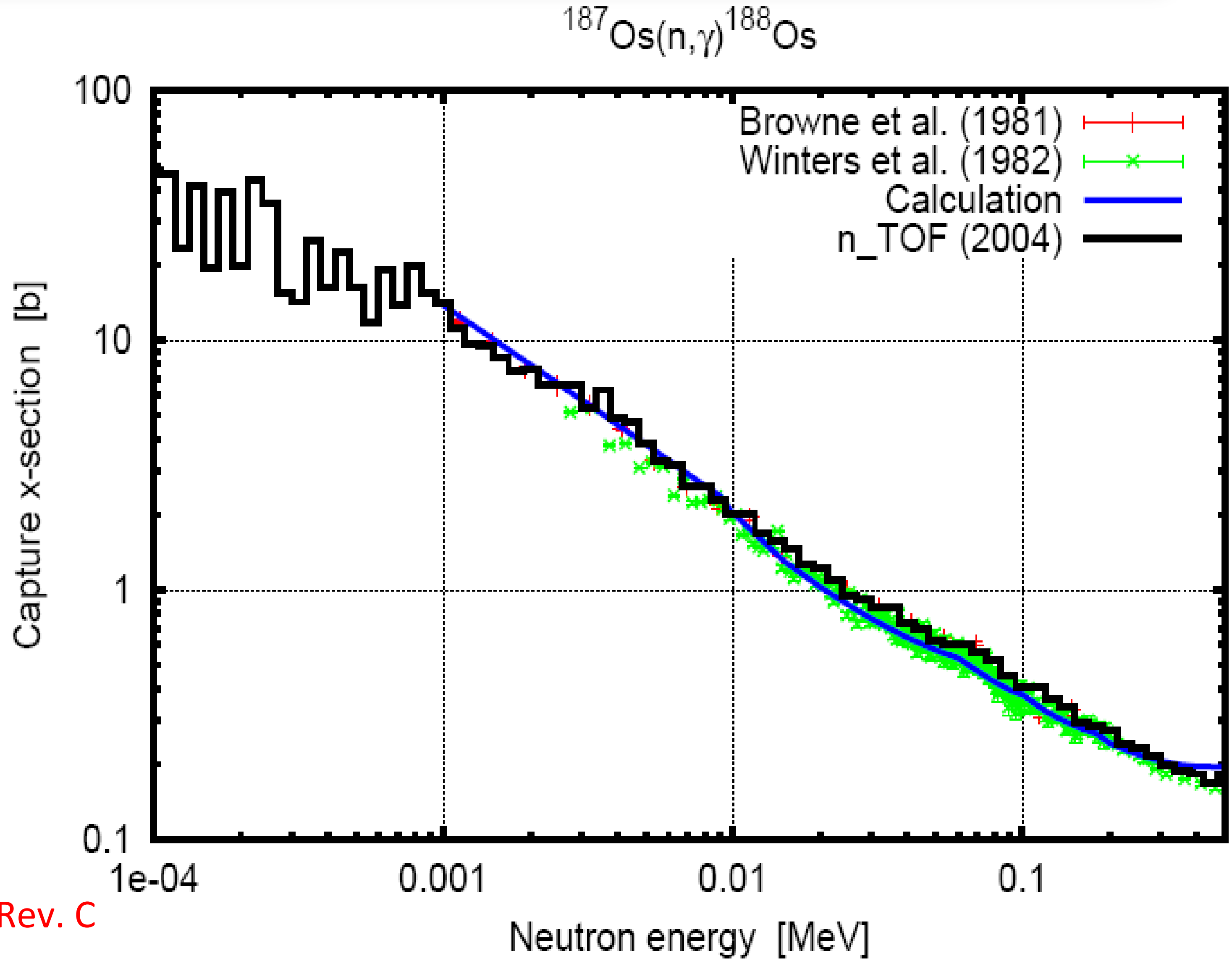

K. Fujii et al.,Phys. Rev. C

Os: implications

- Cosmological way

13.7 ± 0.2 Gyr

- Astronomical way

14 ± 2 Gyr

- Nuclear way: Re/Os clock   Th/U clock

14.9 ± 2 Gyr(*)   **14.5 ± 2.5 Gyr**

(*) 0.4 Gyr uncertainty due to x-sections